International Union of Angiology (IUA) consensus paper on imaging strategies in atherosclerotic carotid artery imaging

Atherosclerosis 354 (2022) 23–40

Contents lists available at ScienceDirect

Atherosclerosis

journal homepage: www.elsevier.com/locate/atherosclerosis

Review article

International Union of Angiology (IUA) consensus paper on imaging strategies in atherosclerotic carotid artery imaging: From basic strategies to advanced approaches☆

Luca Saba [a,*], Pier Luigi Antignani [b], Ajay Gupta [c], Riccardo Cau [a], Kosmas I. Paraskevas [d], Pavel Poredos [e,ab], Bruce A. Wasserman [f], Hooman Kamel [g], Efthymios D. Avgerinos [h,ac], Rodrigo Salgado [i], Federico Caobelli [j], Leonardo Aluigi [k], Luis Savastano [l], Martin Brown [m], Tom Hatsukami [n], Emad Hussein [o], Jasjit S. Suri [p,ad,ae], Armado Mansilha [q], Max Wintermark [r], Daniel Staub [s], Jose Fernandes Montequin [t], Ruben Tomas Toro Rodriguez [t], Niranjan Balu [n], Jan Pitha [u], M. Eline Kooi [v], Brajesh K. Lal [w,af], J. David Spence [x], Giuseppe Lanzino [u], Hugh Stephen Marcus [y], Marcello Mancini [z], Seemant Chaturvedi [aa], Ales Blinc [e]

[a] Department of Radiology, Azienda Ospedaliero Universitaria (A.O.U.), di Cagliari – Polo di Monserrato s.s. 554 Monserrato, Cagliari, 09045, Italy
[b] Vascular Center, Nuova Villa Claudia, Rome, Italy
[c] Department of Radiology Weill Cornell Medical College, New York, NY, USA
[d] Department of Vascular Surgery, Central Clinic of Athens, Athens, Greece
[e] Department of Vascular Disease, University Medical Center Ljubljana, Zaloska cesta 2, 1000, Ljubljana, Slovenia
[f] The Russell H. Morgan Department of Radiology and Radiological Science, Johns Hopkins Hospital, 367 East Park Building, 600 N Wolfe St, Baltimore, MD, 21287, USA
[g] Clinical and Translational Neuroscience Unit, Feil Family Brain and Mind Research Institute, Department of Neurology, Weill Cornell Medicine, New York, USA
[h] Division of Vascular Surgery, University of Pittsburgh Medical Center, Pittsburgh, Pa, USA
[i] Department of Radiology, Antwerp University Hospital (UZA), Edegem, Belgium
[j] University Clinic of Nuclear Medicine, Inselspital, University Hospital Bern, Bern, Switzerland
[k] Angiology Care Unit, Private Villalba Hospital (GVM), Bologna, Italy
[l] Neurosurgery, Mayo Clinic, Rochester, MN, USA
[m] Department of Neurology and Neurosurgery, University College London Hospitals, London, UK
[n] Department of Surgery, University of Washington, Seattle, WA, USA
[o] Vascular surgery Department, Ain Shams University, Cairo, Egypt
[p] Monitoring and Diagnostic Division, AtheroPoint™, Roseville, CA, USA
[q] Faculty of Medicine of University of Porto, Porto, Portugal
[r] Department of Radiology, Neuroradiology Section, Stanford University School of Medicine, Stanford, CA, USA
[s] Department of Angiology, University Hospital Basel and University of Basel, Basel, Switzerland
[t] National Institute of Angiology and Vascular Surgery, Havana, Cuba
[u] Laboratory for Atherosclerosis Research, Center for Clinical and Experimental Medicine, Institute for Clinical and Experimental Medicine, Prague, Czech Republic
[v] Department of Radiology and Nuclear Medicine, CARIM School for Cardiovascular Diseases, Maastricht University Medical Center, Maastricht, the Netherlands
[w] Department of Vascular Surgery, University of Maryland, Baltimore, USA
[x] Stroke Prevention & Atherosclerosis Research Centre, Robarts Research Institute, Western University, 1400 Western Road, London, N6G 2V4, ON, Canada
[y] Stroke Research Group, Department of Clinical Neurosciences, University of Cambridge, Cambridge, UK
[z] Institute of Biostructures and Bioimaging, National Research Council of Italy, Naples, 80145, Italy
[aa] Department of Neurology & Stroke Program, University of Maryland School of Medicine, Baltimore, MD, USA
[ab] Faculty of Medicine, University of Ljubljana, Vrazov trg 2, 1000, Ljubljana, Slovenia
[ac] Clinic of Vascular and Endovascular Surgery, Athens Medical Group, Greece
[ad] Knowledge Engineering Center, Global Biomedical Technologies, Inc, Roseville, CA, USA
[ae] Department of Electrical and Computer Engineering, Idaho State University, ID, USA
[af] Vascular Service, Veterans Affairs Medical Center, Baltimore, USA

☆ J. Pitha was supported by Ministry of Health of the Czech Republic, grant No. NU22-02-00051.
* Corresponding author.
E-mail address: lucasaba@tiscali.it (L. Saba).

https://doi.org/10.1016/j.atherosclerosis.2022.06.1014
Received 30 April 2022; Received in revised form 10 June 2022; Accepted 14 June 2022
Available online 28 June 2022

ARTICLE INFO

Keywords:
Carotid artery
Atherosclerosis
US
CT
MRI
PET

ABSTRACT

Cardiovascular disease (CVD) is the leading cause of mortality and disability in developed countries. According to WHO, an estimated 17.9 million people died from CVDs in 2019, representing 32% of all global deaths. Of these deaths, 85% were due to major adverse cardiac and cerebral events. Early detection and care for individuals at high risk could save lives, alleviate suffering, and diminish economic burden associated with these diseases.

Carotid artery disease is not only a well-established risk factor for ischemic stroke, contributing to 10%–20% of strokes or transient ischemic attacks (TIAs), but it is also a surrogate marker of generalized atherosclerosis and a predictor of cardiovascular events. In addition to diligent history, physical examination, and laboratory detection of metabolic abnormalities leading to vascular changes, imaging of carotid arteries adds very important information in assessing stroke and overall cardiovascular risk. Spanning from carotid intima-media thickness (IMT) measurements in arteriopathy to plaque burden, morphology and biology in more advanced disease, imaging of carotid arteries could help not only in stroke prevention but also in ameliorating cardiovascular events in other territories (e.g. in the coronary arteries).

While ultrasound is the most widely available and affordable imaging methods, computed tomography (CT), magnetic resonance imaging (MRI), positron emission tomography (PET), their combination and other more sophisticated methods have introduced novel concepts in detection of carotid plaque characteristics and risk assessment of stroke and other cardiovascular events. However, in addition to robust progress in usage of these methods, all of them have limitations which should be taken into account. The main purpose of this consensus document is to discuss pros but also cons in clinical, epidemiological and research use of all these techniques.

1. Current scenario and evidence

1.1. Targets of carotid imaging

Detailed imaging assessment of extracranial carotid artery disease is critical for appropriate risk stratification and management of those presenting with cerebrovascular ischemia as well as of selected asymptomatic individuals [1].

The degree of luminal stenosis in the carotid bifurcation has historically served as the primary imaging feature for determining ischemic stroke risk and the potential need for surgery. Contemporary multimodality imaging including ultrasound, magnetic resonance imaging (MRI/MRA), CT angiography (CTA), and even positron emission tomography (PET-CT) or PET-MRI methods target more detailed visualization of carotid plaque components that indicate plaque vulnerability (e.g. maximum plaque thickness and volume, calcification, ulceration, intraplaque hemorrhage, inflammation, intraplaque neovascularization, lipid-rich necrotic core, and thin or ruptured fibrous cap) [1] (Table 1).

Not infrequently a carotid scan can indirectly (through flow patterns) detect the status of other vascular territories or even other abnormal findings of surrounding structures (e.g. a thyroid nodule) [2].

1.2. The role of carotid arteries imaging

There are several reasons that require carotid imaging, the predominant being evaluation after a cerebrovascular event but also for CVD screening, risk stratification, and prevention as well as for surveillance after a carotid procedure [1,3].

Imaging of the carotid bifurcation is essential in all patients with symptoms of cerebral ischemia, whether they present as a TIA or complete stroke [1,3]. If significant carotid artery disease is identified as the source of symptoms, these patients are candidates for a carotid intervention to prevent a secondary stroke [3]. Although imaging for this indication is most often performed with a carotid duplex ultrasound, when evaluation of the vessels proximal or distal to the cervical portion of the carotid artery is required for diagnosis or to plan endovascular or surgical therapy, additional imaging with CTA, MRA or digital subtraction angiography (DSA) is indicated [3].

The use of imaging methods for screening for carotid artery disease in the general population, in particular, to identify significant disease that will prompt an intervention to prevent a stroke are controversial [3]. However, targeting selected groups of neurologically asymptomatic patients is well established. These groups can be high-risk patients aged >55 years with cardiovascular risk factors, patients with a carotid bruit on clinical exam, Hollenhorst plaque on fundoscopic examination, and silent infarction on brain imaging examinations [3].

Finally, surveillance after a carotid intervention is a common practice established on the natural history of ipsilateral restenosis, contralateral disease progression, and associated stroke risk.

2. Ultrasound

2.1. Stenosis

Grading and stratification of carotid stenosis is manly based on multiparametric, hemodynamic criteria on Duplex ultrasound [4] (Table 2). The most important parameters are the measurement of the peak systolic and the end-diastolic flow velocity within the stenosis. The accuracy of Duplex ultrasound compared with angiography for detecting >50% and ≥70% stenosis, respectively, is very good, with a positive predictive value of >90% and a specificity of >85% [5]. Duplex ultrasound is recommended as the primary imaging modality to assess the

Table 1
Main imaging methods for carotid arteries.

	Atherosclerosis vulnerable plaque	Accuracy	Sensitivity	Burden	Availability	Standardization
Ultrasound	++ + -	+	+++	-	+++	+ -
CT angiography	++ - -	++	++	++	+ -	++
Magnetic resonance	+++ ++	++	+++	-	- -	+ -
Positron emission tomography	+++ +++	+	+++	+	- - -	+ -

Table 2
(Duplex-)sonographic criteria for grading internal carotid artery stenosis and markers of carotid plaque vulnerability.

Sonographic marker	Classification/Feature of plaque vulnerability
Grading of internal carotid artery stenosis based on Duplex ultrasound	Degree of stenosis as defined by NASCET - < 50%: plaque on B-mode, aliasing on color duplex image, PSV <200 cm/s - 50–69%: PSV 200–300 cm/s, EDV <100 cm/s, PSV ratio (ICA/CCA) ≥ 2 - ≥70%: PSV >300 cm/s, EDV >100 cm/s, PSV ratio (ICA/CCA) ≥ 4 Progression of degree of stenosis (>20%)
Echogenicity on B-mode ultrasound	Hypoechogenic (echolucent) plaque (type 1 or type 2) «Grey scale median (GSM)»: GSM <15 (hypoechogenic) Increased juxta-luminal hypoechogenic (black) area (>6 mm^2) Heterogenic echotexture
Plaque burden on B-mode ultrasound including 3D-ultrasound	Large plaque area (>40 mm^2)/total plaque area Large plaque volume/total plaque volume (3D-ultrasound)
Carotid plaque surface on Duplex-ultrasound and CEUS	Plaque surface irregularities (<1–2 mm) Plaque ulceration (>1–2 mm)
Carotid intraplaque neovascularization (IPN) on CEUS	Increased IPN on semi-quantitative measurement: • grade 1: no vascularization • grade 2: limited or moderate vascularization • grade 3: extensive vascularization High IPN on semiautomatic quantitative measurement: e.g. large relative perfused area

Peak systolic flow velocity (PSV), end-diastolic flow velocity (EDV), contrast-enhanced ultrasound (CEUS).

extent and severity of extracranial carotid stenosis [6]. Various studies have also shown that the risk of cerebrovascular events increases not only with the severity of the stenosis but also with rapid progression of the degree of stenosis [7,8]. Therefore, patients with an asymptomatic carotid stenosis (ACS) undergo usually annual ultrasound monitoring.

2.2. Features of vulnerability

Duplex ultrasound can assess not only the degree of stenosis [4,9], but also several sonomorphological characteristics which are associated with plaque vulnerability [10]. Hypoechogenicity including a low grey scale median (GSM) [11,12], large juxtaluminal hypoechogenic area [13], heterogeneous echotexture [14,15], or higher plaque burden (plaque area, total plaque area [TPA], or plaque volume) [16,17], surface irregularities and ulceration [14] on B-mode ultrasound are sonographic features of plaque vulnerability with increased embolic risk [6] (Table 2).

IMT represents mainly the middle layer of the carotid arterial wall and is a marker of arteriopathy [18].

According to the American Society of Echocardiography, IMT is a subclinical vascular disease rather than synonymous of subclinical atherosclerosis [19]. A 2020 review article summarized many of the advantages of measuring carotid plaque burden, which is far superior to measuring carotid IMT in many ways [16].

Carotid plaque burden (CPB) is useful for risk stratification, treatment of atherosclerosis, research into the biology and genetics of atherosclerosis, and evaluation of new therapies against atherosclerosis.

Measured as TPA or as 3D plaque volume, CPB is highly correlated with coronary calcium [17], and as predictive of events [20]; while IMT is neither [17,20]. A recent study reported that CPB was superior to coronary calcium for risk stratification in women [21]; it is also detected at a younger age. CPB also has significant advantages compared with coronary calcium, because it can be measured repeatedly, to assess and adjust the effects of therapy. Serial assessment of plaque burden in conjunction with life-style and pharmacological treatment according to guidelines, called "Treating Arteries" (instead of merely treating risk factors), markedly improves therapy for atherosclerosis. In part this is because showing patients images of their plaque markedly improves compliance with lifestyle changes and medication [22]. Among high-risk patients with asymptomatic carotid stenosis, implementation of "Treating Arteries" was associated with a >80% reduction of the 2-year risk of stroke/myocardial infarction/vascular death [23]. In prevention clinics across Argentina, "Treating Arteries" was implemented in 2010; among patients age >65, the annual risk of cardiovascular events declined from 5.85% to 2.35% between 2011 and 2015 [24]. Patients in Germany who were treated with lipid-lowering drugs on the basis of a high CPB had a much lower risk of cardiovascular events over 3.9 years, than patients treated only on the basis of serum cholesterol: (5.4% vs 23%, respectively) [25]. It has been supported that "Treating arteries" without measuring plaque would be like treating hypertension without measuring blood pressure." [26].

Studies using CPB identify new causes of atherosclerosis, either through genetic studies [27], or studies of new risk factors such as toxic metabolites produced by the intestinal microbiome [28]. Such studies will lead to new therapies for atherosclerosis, and measurement of CPB markedly reduces sample size and duration of studies to evaluate such new therapies [29].

New automated methods based on machine learning for measuring TPA for measuring TPA, 3D carotid plaque burden [30] and Vessel Wall Volume [31] (which can be measured in persons without plaque, so it can replace IMT) will make it much easier to implement this. These new methods are very fast, reliable, and reproducible [32]. Fig. 1 shows comparisons of automated with manual segmentation.

2.3. Transcranial Doppler detection of embolic signals in carotid artery disease

Transcranial Doppler ultrasound (TCD) is a non-invasive technique that can be used to detect circulating emboli/intracranial embolism. These emboli appear as short-duration, high-intensity embolic signals/intracranial embolism and are accompanied by a characteristic chirping sound. TCD circulating emboli detection has been shown to have a high sensitivity and specificity in experimental studies [33], although in clinical practice care needs to be applied in distinguishing true embolic signals (also known as high-intensity transient signals) from artefact. Consensus criteria have been developed to allow this [34].

Studies have demonstrated that there were differences in the prevalence of embolic signal in the different stroke subtypes with a higher occurrence in large artery stroke in comparison with cardioembolic and lacunar stroke [35]. In patients with recently symptomatic carotid stenosis (SCS), during a 1-h recording from the ipsilateral middle cerebral artery (MCA) embolic signals can be identified in about 40% of individuals [36]. A higher prevalence has been reported in patients with more recent symptoms, SCS compared with ACS, and plaque imaging characteristics indicate a higher risk plaque [37].

Prospective longitudinal studies have demonstrated that asymptomatic embolization encountered by TCD predicts future stroke risk in both SCS [36] and ACS [38–42].

The effect is additive to that obtained by plaque imaging modalities such as carotid ultrasound [43]. It has been suggested that embolic

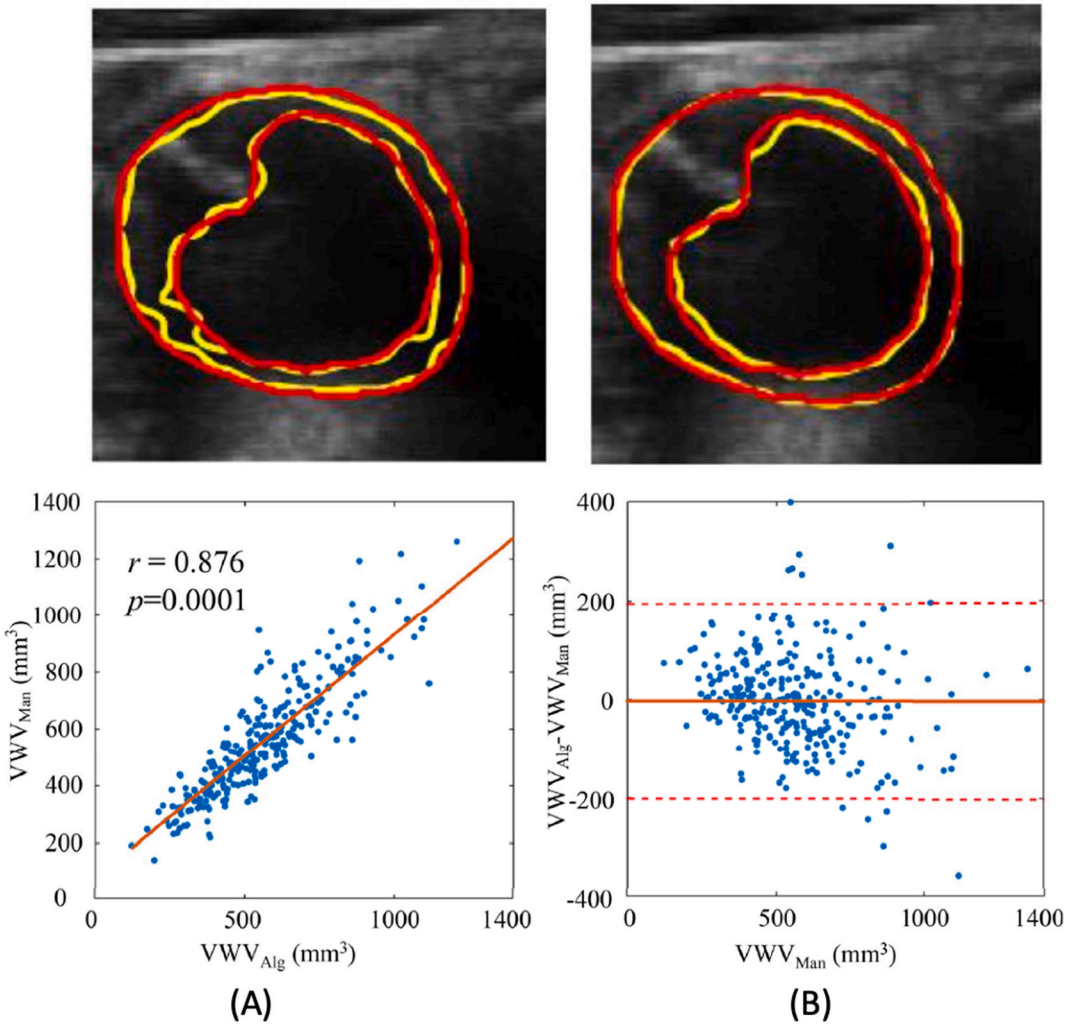

Fig. 1. Automated measurement of vessel wall volume.
(A) Automated segmentation (yellow line) was very accurate compared to manual segmentation by experts (red line). Dice-similarity-coefficient (DSC) was 93.2 ± 3.0% for the Medial-Arterial Boundary in the common carotid artery and 91.9 ± 5.0% in the bifurcation. DSC for the Lumen-Intima Boundary was 89.5 ± 6.7% and 89.3 ± 6.8% for the Common Carotid Artery and the bifurcation respectively. Automated segmentation took less than 1 s for each side. (B) Relationships of the automated and manual VWV measurements for n = 302 3DUS images in the CAIN dataset. (a) Linear correlation (r = 0.876, $p = 0.0001$), and (b) Bland-Altman plot of the two sets of VWV measurements. The solid red line and the dash red lines represent the bias (−3.6 mm^3) and mean ± 1.96 SD, respectively. Reproduced by permission of IEEE from: Zhou R, Guo F, Azarpazhooh MR, Spence JD, Ukwatta E, Ding M and Fenster A. A Voxel-Based Fully Convolution Network and Continuous Max-Flow for Carotid Vessel-Wall-Volume Segmentation From 3D Ultrasound Images. IEEE Trans Med Imaging. 2020; 39:2844–2855. (For interpretation of the references to color in this figure legend, the reader is referred to the Web version of this article.)

signal detection may be a useful method to identify ACS patients at high risk who may particularly benefit from carotid endarterectomy (CEA) [41] although this needs to be proven in a randomized intervention study. Conversely, patients with an absence of embolic signals may do well with intensive medical management alone.

Embolic signal detection has been used to evaluate the effectiveness of antithrombotic drugs in carotid artery disease [40]. Studies have shown that aspirin, clopidogrel but also statins reduce embolic signals [40,44,45]. Combination antiplatelet regimens such as aspirin and clopidogrel were more effective than aspirin alone in randomized controlled trials [40,46]. This paralleled subsequent studies demonstrating their greater effectiveness in preventing recurrent stroke after minor stroke and TIA [44,46], and reinforcing the evidence that embolic signal detections may be a useful surrogate marker to identify the efficacy of antithrombotic agents.

2.4. Impact of contrast material

As a complement to conventional duplex ultrasound, intravenous application of ultrasound contrast agents has greatly enriched sonographic imaging in vascular medicine [47,48]. Contrast agents consist of small microbubbles, which circulate strictly intravascularly in the bloodstream for several minutes after application. Due to their non-linear reflection pattern, a contrast-specific ultrasound image is obtained, which enhances not only the vessel lumen but also the microcirculation in the vessel wall (vasa vasorum) including intraplaque neovascularization (IPN) [49].

In the carotid artery, contrast-enhanced ultrasound (CEUS) is helpful in distinguishing complete vessel occlusion from very high-grade carotid stenosis. In addition, particularly hypoechogenic plaques can be well detected and surface irregularities and ulcerations of arteriosclerotic lesions can be better delineated [50–52]. The most important value of CEUS lies in the detection and quantification of IPN [48], which is usually performed semiquantitatively [53,54]. Such visual-based

quantification has good intra- and interobserver variability, but a more objective, purely quantitative measurement of IPN ranging from measurements of maximal contrast enhancement to automated, computer-assisted quantification of the relative perfused area is desirable [55–57].

IPN on CEUS has been compared with the corresponding vascularization on histopathologic examination in patients with carotid stenosis before CEA showing a good correlation between the IPN and the extent of microvessels and inflammation within the plaque on histology [58–60].

It has been demonstrated that hypoechogenic plaques, which were considered vulnerable on B-mode ultrasound, had higher IPN on CEUS than the more stable hyperechogenic lesions [53,58]. Various retrospective studies of patients with carotid plaque revealed that those lesions with a higher embolic risk had increased plaque IPN on CEUS imaging. Thus, it was shown in a meta-analysis that the prevalence of IPN was higher in SCS compared with ACS patients [15] and correlates with cardiovascular events [61]. Different prospective studies also demonstrated that in patients with a recent ischemic cerebrovascular event the risk of future ischemic stroke or TIA was significantly associated with IPN in carotid CEUS examination [62,63]. IPN on CEUS imaging was also found to be predictive of significant and complex coronary artery disease and future cardiovascular events [64].

Carotid CEUS examination has the potential to improve risk stratification with respect to the occurrence of embolization by grading IPN in patients with carotid plaque and stenosis. This could be useful to monitor therapeutic interventions [65] and to better select patients with carotid stenosis, who benefit from a possible invasive therapy [49].

3. Computed tomography

3.1. Stenosis

CTA has evolved along with the technological advances of CT hardware and software. Modern CTA, performed with multidetector high-speed CT hardware and evaluated with 3D reformatting software, accurately and reliably depicts carotid disease and allows for direct quantification of carotid stenosis in millimeters [66–72].

CTA is an anatomic study of arteries, allowing for direct evaluation of carotid stenosis. CTA is fast, with images of the head and neck acquired over approximately 5–15 s during contrast injection. 512 × 512 memory matrix multidetector CT scanners allow acquisitions with near-isotopic spatial resolution and an effective section thickness as small as 0.5 mm [73]. For evaluation of carotid arteries and the cerebral vasculature, it is possible to narrow the nominal section thickness to obtain a submillimetric dataset. This ability, combined with 3D image rendering, provides excellent accuracy for the measurement of the degree of stenosis [73]. In light of the relative benefits of CTA in reference to safety, time, and related lower cost than DSA, it is compelling to use CTA when the indication for angiography is not to deliver a therapeutic intervention such as stenting but to accurately characterize the degree of stenosis. Venous filling is not an artefact for neck carotid imaging, because arteries are easily recognized as distinct from veins.

CTA evaluation is mainly based on axial sections and curved planar reformations (CPR). CTA has been shown to have a pooled sensitivity of 95% and specificity of 98% for the detection of >70% stenoses [74]. There are advantages of quantifying carotid stenosis by direct millimeter measurements instead of or in addition to the well-known North American Symptomatic Carotid Endarterectomy Trial (NASCET)–style ratio calculations [75]. Multi-slice CTA can in addition detect tandem stenoses in the region of the carotid origin from the aorta, the carotid siphon, and the intracranial portion of the carotids. CT is able to provide a comprehensive evaluation of patients with acute stroke by using a combined approach of pre-contrast CT to detect hemorrhage and manifest infarction, perfusion CT measurements to differentiate between penumbra and infarct, and CTA to detect the occluded vessel as well as potential concomitant carotid abnormalities.

3.2. Features of vulnerability

Atherosclerotic disease is a complex, heterogeneous, and multifactorial condition with several types of components in the same plaque. The role of plaque imaging is to identify those imaging biomarker features of carotid plaque that are related to vulnerable plaque [76–79]. In particular, CTA thanks to its spatial resolution is able to assess the carotid artery lumen and the arterial wall.

A key feature of vulnerable carotid plaque is Intraplaque hemorrhage (IPH), which is defined by the accumulation of blood components within the carotid plaque [80]. Regarding the pathogenesis of IPH, most of the authors suggest that it is linked to the rupture of neovessels or plaque rupture itself, and some trigger events including inflammation, metabolic diseases or diabetes may precipitate this condition [80]. IPH represents the strongest imaging feature associated with the occurrence of stroke [81], and it is also more common in carotid artery ipsilateral to embolic stroke of undetermined source [82]. Conflicting results have been reported about the role of CT to detect this feature. However, studies suggest that CTA is able to discriminate the presence of IPH, both directly according to attenuation at 25 HU [83] and indirectly with the presence of calcified rim and soft internal plaque [84].

The thin fibrous cap with a lipid-rich necrotic core (LRNC) represents one of the most important features of the carotid artery vulnerable plaque model. In particular, LNRC is considered a collection of heterogeneous tissue composed of cholesterol crystals and necrotic debris of apoptotic cells [85].

The fibrous cap is a layer of fibrous connective tissue that contains macrophages and smooth-muscle cells, and particularly the morphology and thickness of the fibrous cap are indicative of rupture [86]. These two imaging features are associated with the risk of stroke, especially when a thin fibrous cap covers a large LRNC [87].

In addition, the LRNC size correlates with future ipsilateral carotid symptoms [88]. CT can be used to visualize lipid components of the LNRC, thanks to lipid tissue attenuation properties, but may more hardly discriminate between LRNC and IPH, given the attenuation values of these two features [88]. Similarly, the evaluation of the fibrous cap with CT is not considered optimal because of the artefact related to halo-effect and edge-blur [89].

Another feature of plaque vulnerability is inflammation of the carotid artery plaque. Different types of inflammatory cells have been identified in the carotid plaque usually located in the plaque shoulder, cap, or both with a role in plaque “instability” [89,90]. Beyond the presence of macrophages, plasma cells are also associated with the risk of rupture and the occurrence of cardiovascular events [90].

Similarly, plaque neovascularization is considered a marker of plaque vulnerability, which is related to newly formed neovessel arising into the intima and is associated with plaque activity [88]. The presence of neovascularization in carotid plaque represents an element of instability because these microvessels are prone to rupture due to their immature and imperfect endothelial structure [91]. CTA can identify the presence and the degree of neovascularization thank its ability to detect contrast plaque enhancement [92].

Beyond plaque composition, vulnerable plaques tend to be associated with plaque surface morphology (i.e. smooth, irregular, or ulcerated) [77]. In particular, the presence of ulceration, defined as an intimal defect larger than 1 mm in width [88], is considered a risk feature for cardiovascular events [93]. The carotid plaque surface morphology can be better assessed with CTA in comparison with other

Table 3
CT features of plaque vulnerability and its strengths and limitations.

	Imaging features	Supporting evidence	Limitations	General limitations
Intraplaque hemorrhage	Directly: attenuation values ≤ 25 Indirectly: calcified rim and soft internal plaque	Moderate supporting evidence	Similar HU attenuation values between soft plaque components	•Radiation dose delivered to the patients •Potential side effect
Lipid-rich necrotic core	Presence of soft plaque components	Conflicting supporting evidence	Artefact related to halo-effect and edge-blur	•The limit tissue constrast between soft plaque components
Plaque inflammation	Presence of contrast plaque enhancement	Weak supporting evidence		•Overstimates the degree of the stenosis due to calcium deposits
Neovascularization	Presence of contrast plaque enhancement	Moderate supporting evidence		
Plaque surface morphology	Alterations of the luminal surface on the luminal profile of the plaque	Strong supporting evidence	Presence of a halo or edge blur may hinder detection of smaller ulcerations	
Plaque volume and composition	Size of the carotid plaque with its subcomponents	Strong supporting evidence	Limit tissue contrast attenuation in some plaque subcomponents	
Calcifications	Size and morphology of calcium deposits	Strong supporting evidence		

non-invasive imaging modalities, as demonstrated by Saba et al. [94,95].

Also, carotid plaque volume is a crucial determinant of plaque vulnerability. Rozie et al. demonstrated that plaque volume and the relative subcomponents of the plaque are associated with plaque vulnerability and stroke [96]. Thanks to its excellent spatial resolution, CTA can easily evaluate this parameter [76].

Among the multiple parameters that have been indicated as responsible for an increased vulnerability, conflicting results have emerged in the identification of a role for calcium. Emerging research has suggested various mechanisms in calcium deposition leading to different phenotypes of carotid plaque calcification [97–101]. Yang et al. investigated the association between calcium configurations and ulceration with IPH, demonstrating that superficial, multiple, and thin calcifications were associated with IPH. The authors concluded that the size and location may represent a marker of high-risk plaque [98]. Table 3 summarizes the CT features of plaque vulnerability and its strengths and limitations.

3.3. Ancillary findings in carotid imaging

While evaluation of vessel patency and plaque characteristics remains the main reason to perform CT/MR-imaging of the carotid arteries, a variety of ancillary findings can be encountered (Table 4). Some are merely incidental findings with no further clinical relevance, while others represent a different etiology of the patient's complaints with clear implications for further treatment and prognosis. Although a detailed scope of all possible ancillary findings is outside the scope of this paper, some important entities will now further be discussed.

3.3.1. Carotid dissection

As in the aorta, a dissection of the carotid artery wall constitutes a disruption of the carotid intima layer, with blood flowing into the vessel wall and the creation of a true and false lumen [102].

A carotid artery dissection can be spontaneous or post-traumatic [102]. When spontaneous, an underlying condition must be ruled-out, which can include entities like fibromuscular dysplasia, Marfan syndrome, and Ehler-Danlos syndrome [102,103]. It is important to scrutinize the other cervical arteries as well, as they may exhibit morphological changes contributing to a correct diagnosis (e.g. signs of fibromuscular dysplasia in the contralateral artery) [104].

The pathophysiology of a carotid dissection explains its imaging findings [103]. In contrast to the aorta, the dissection flap is seldom seen in a carotid artery dissection, as the false lumen usually thromboses and creates a semicircular non-enhancing soft tissue density surrounding the true lumen (Fig. 2) [103]. This makes MR-imaging especially useful, as this thrombus will lead to a hyperintense signal on fat-suppressed T1-weighted images due to blood breakdown products. It can be problem-solving in cases in which the presence and extent of the dissection can be difficult to assess on CT alone, as the difference in contrast between the wall hematoma and surrounding tissues can be limited [103].

A carotid dissection usually appears in the supra-bulbar internal carotid artery. In many cases, it will remain limited to the extracranial segment, but extension into the skull base can occur [103,104].

3.3.2. Carotid web & thrombus

A carotid web is identified as a small, (curvi)lineair soft tissue density protruding into the carotid lumen usually at the level of the carotid bulb [105,106]. According to some authors, it represents a variant of fibromuscular dysplasia and is associated with an increased risk for stroke, especially in younger patients without classic vascular risk factors [107].

A thrombus presents as a non-enhancing central structure surrounded by flowing blood (the so-called "donut" sign). While rare, its presence is important as it is associated with an increased risk for stroke, but also with conditions leading to a hypercoagulable state like malignancy, infections, and pregnancy [105,106].

3.3.3. Inflammatory and infectious conditions

Carotid vasculitis can be defined as the inflammation of carotid artery walls with or without necrosis, leading to stenosis or occlusion of

Table 4
Ancillary findings.

Condition	Comments
Congenital	Agenesis, aplasia or hypoplasia of ICA
Inflammatory & infectious conditions	Carotidynia
	Giant cell arteritis
	Takayasu arteritis
	Post-radiation arteritis
Carotid dissection	Traumatic or spontaneous
	Consider underlying condition with spontaneous (e.g. FMD)
Carotid web & floating thrombus	Associated with increased stroke risk

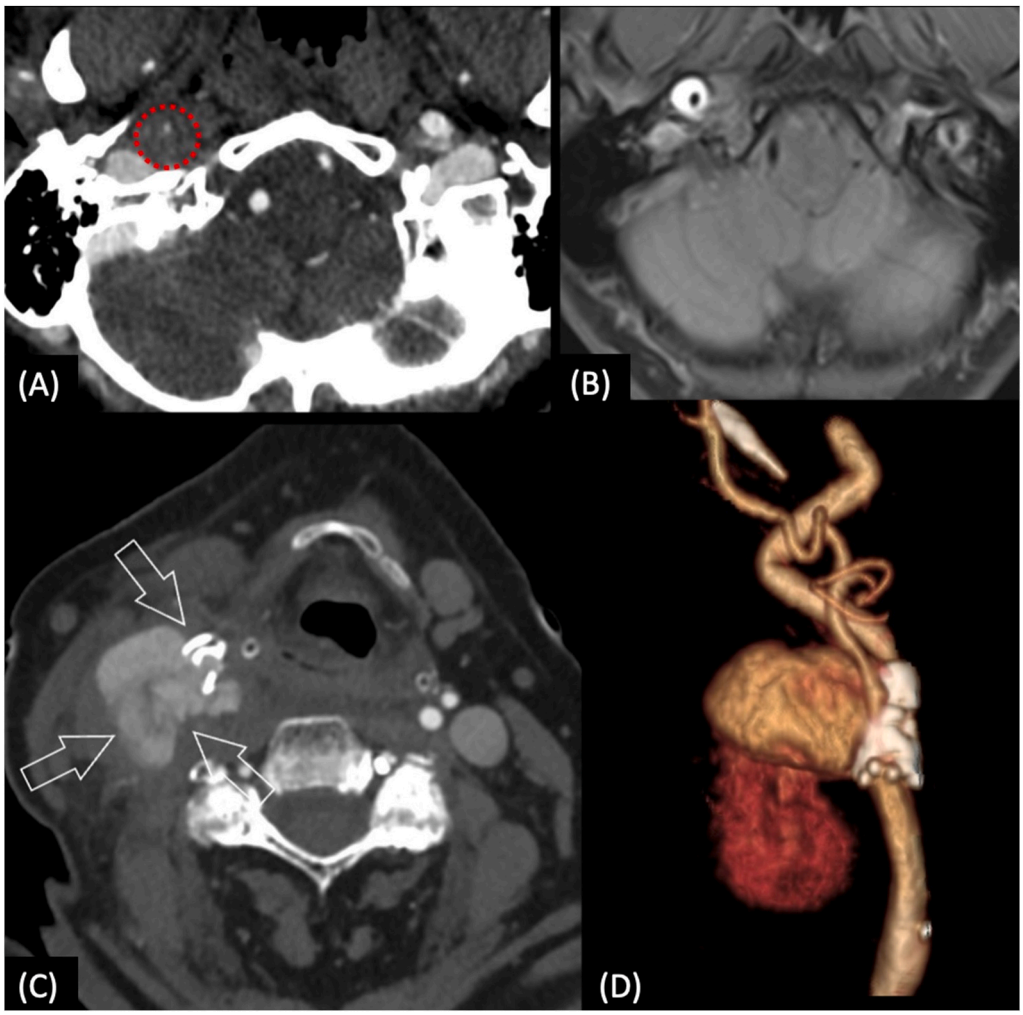

Fig. 2. Carotid artery dissection (A and B) in a 49-year-old female patient.
The CTA shows the filiform lumen in the right ICA (A) that is confirmed by the MR B). Infective pseudo-aneurysm in 63-year-old male patient (C and D). The CTA shows the contrast material due to into the pseudoaneurysm (white open arrows, C) and the volume rendered image (D) confirms the spatial relationship.

the lumen [108]. Vasculitis may be associated with systemic connective tissue disorders or may be secondary to infection, malignancy, drugs, or radiation therapy [108]. For a correct diagnosis, relevant laboratory tests are also required. The 2012 Chapel Hill Consensus Conference defined different types of vasculitis in terms of (a) the size of the involved arteries and (b) associated pathologic lesions [109]. The most frequent vasculitis involving carotid arteries are Takayasu arteritis and Giant cell arteritis [108,109]. Infectious extracranial carotid disease is rare and usually caused by *Staphylococcus aureus*, Salmonella, and streptococcus species. When present, it can manifest as an infected aneurysm with a focal weakinging of the wall, development of a pseudo-aneurysm, and increased rupture risk (Fig. 2).

With CTA/MRA imaging, signs of carotid vasculitis are vessel wall thickening (mostly concentric representing a key parameter in the differential diagnosis) and contrast enhancement. Usually there is no preference for the involvement of the carotid bifurcation (different from atherosclerotic disease). In the case of active vasculitis contrast enhancement of the thickened vessel wall may be seen on both CT and MR [108].

3.3.4. Other

Any other condition or anomaly that is encountered during a carotid examination must be reported. These include rare instances like carotid body tumours or any other condition that influences clinical management.

4. Magnetic resonance imaging

4.1. Stroke risk assessment and characterization of low-grade carotid atherosclerosis

Risk assessment of carotid atherosclerotic plaque for cerebrovascular ischemic events has historically relied on angiographic measures of stenosis, with thresholds for revascularization defined by randomized clinical trials that date back to the early 1990's [93,110,111]. The established threshold for SCS is 70%, although revascularization is often considered for stenosis beginning at 50% when symptomatic and 60% when asymptomatic [93,110,112,113]. Stenosis has worked well in these studies considering it is a surrogate for plaque burden, which is strongly associated with ischemic stroke risk [16]. However, there have been substantial technical advances in our ability to identify features of atherosclerotic plaque that can improve our precision for stratifying risk [114–116]. This is especially important for atherosclerotic plaques that fall under the thresholds for angiographic detection of risk. Risk estimation for stroke from a plaque causing less than 50% stenosis must be a priority considering the high prevalence of low-grade carotid stenosis in the community [116]. For example, in the Cardiovascular Health Study detectable carotid stenosis was present in 62% of women and 75% of men aged ≥65 years, with only 7% of men and 5% of women having stenosis ≥50% [117]. Risk analysis of carotid plaque must also consider the accommodation of atherosclerotic plaque formation by

flow-mediated outward remodeling regulated by endothelial cells to preserve lumen caliber. This endothelial response is overcome once plaque size reaches a threshold and angiographic stenosis becomes detectable. For example, there is evidence that angiographic narrowing of the extracranial internal carotid artery is not detected until plaque burden reaches 61.9% [118] or 63.1% [119] area stenosis measured on black blood MRI exams, highlighting the large burden of plaque that can exist in low-grade carotid atherosclerosis.

4.2. High-risk carotid plaque features detectable on MRI

Based on histopathologic validation studies [120], MRI has been shown to have high accuracy in detecting key high-risk carotid plaque features. For example, using a multi-sequence protocol with a carotid coil, MRI can identify the presence of an LRNC, thinning/rupture of the fibrous cap, ulceration, and IPH, all of which are strong predictors of future stroke risk [114]. Although the literature strongly supports a potential role for multi-contrast, multi-sequence MRI to aid in risk stratification before stroke and identify culprit lesions after stroke, adoption of these techniques has been limited in the context of acute stroke imaging due to exam length, need for dedicated coil hardware and/or gadolinium, and complexity in image interpretation [121].

In recent years, converging evidence has identified the use of a single T1-weighted, fat-suppressed sequence to identify IPH as a particularly valuable imaging strategy to incorporate into clinical practice [122]. This sequence includes an inversion pulse to suppress the blood in the lumen. In such an approach, IPH can be identified by the presence of T1-hyperintense signal within carotid plaque when noted to be brighter than the signal intensity of adjacent background skeletal muscle [123,124]. A recent meta-analysis of individual patient data of 560 patients from 7 cohort studies showed the annualized rate of ipsilateral stroke in those with carotid IPH to be markedly increased compared to those without IPH across all stenosis severity levels, including those with <50% stenosis [125]. For this reason, MRI-based IPH identification has significant promise not only in identifying patients who may benefit the most from surgical revascularization procedures, but also in identifying culprit low-grade plaques responsible for ischemic strokes which would otherwise be characterized as cryptogenic in nature [126,127]. Patients with an absence of IPH may do well with intensive medical management alone. Given the promise of carotid IPH as a clinically useful MRI risk marker, randomized stroke prevention trials using IPH as a selection criterion will be needed to establish whether there is evidence to support the widespread adoption of this approach in clinical treatment decision-making.

4.3. Role of MRI in assessment of intracranial carotid and aortic arch atherosclerosis

MRI technology has been shown to have an increasing clinical role in the evaluation of atherosclerotic plaques in locations other than the extracranial carotid artery. MRA has high sensitivity and specificity for identification of stenoses >50% involving the intracranial ICA [128,129] and the MCA [130]. It is routinely utilized in clinical practice to identify patients suspected of harboring intracranial stenosis. Limitations of intracranial MRA include long acquisition times and overestimation of the degree of stenosis because of flow artefact.

A major advantage of MRI sequences in the assessment of intracranial plaques is the concomitant acquisition with parenchymal brain imaging. Recent MRI techniques also allow for further characterize plaque composition and its hemodynamic effects. High-resolution vessel wall MRA provides further characterization of the intracranial arterial wall and pathology by suppressing signal from intravascular blood. It is increasingly used to differentiate among different causes of intracranial steno-occlusive disease and to identify/characterize plaques causing minimal or no narrowing on luminal imaging in patients with otherwise unexplained ipsilateral stroke [131–134]. The hemodynamic effects of intracranial plaques can be measured with quantitative MRA which combines traditional MRA-Time-of-Flight (TOF) and contrast-enhanced (CE)-MRA. This technique allows quantification of the hemodynamic significance of a plaque, which may not necessarily correlate with the degree of narrowing [135].

Aortic arch atheroma has been recognized as a potential cause of emboli in patients with cryptogenic stroke and MRI-based multicontrast plaque imaging was used to recognize vulnerable aortic arch plaques [136]. The addition of 4D flow measurements identifies potential embolization pathways to the brain and is especially useful to suggest possible retrograde embolization in patients with vulnerable plaques located in the proximal descending aorta immediately distal to the origin of the large extracranial arteries [136].

5. Other techniques

5.1. PET

PET enables molecular imaging of biological and biochemical processes in vivo, whereas hybrid PET/CT [137] or PET/MRI [138,139] also provides additional information on plaque morphology. The glucose analogue 18F-Fluorodeoxyglucose (FDG) is taken up by cells with a high metabolic rate, such as macrophages within an atherosclerotic plaque, and therefore enables to quantify the inflammatory activity within carotid atherosclerotic plaques [140]. In order to correct for uptake of the tracer in the blood pool, it is recommended to use the target to background ratio (TBR) to quantify FDG uptake [141]. TBRmax is defined as the ratio of the maximal standardised uptake value (SUVmax) measured in the plaque and the mean SUV (SUVmean) in the blood pool [141]. In a study of 49 patients that underwent an 18F-FDG PET examination before CEA, it was shown that the TBRmax correlates with the extent of CD68 staining, a measure for macrophage content of the plaque ($r = 0.51$, $P < 0001$) (Fig. 3) [142]. Various studies demonstrated higher uptake in symptomatic compared to asymptomatic plaques, while the activity in symptomatic plaques decreases in the months after the event [142–146]. Moreover, several studies reported weak correlations between 18F-FDG uptake on PET and CT/MRI parameters of carotid plaque (Spearman ρ: 0.098–0.39), indicating that PET may have additive information for risk assessment [143,147,148]. Importantly, 18F-FDG uptake was demonstrated to predict early post-PET stroke recurrence with a fully adjusted hazard ratio of 4.57 (95% confidence interval [CI], 1.5–13.96; $p = 0.008$) in a pooled cohort of 196 patients with carotid stenosis and recent stroke/transient ischemic attack with 8 post-PET stroke recurrences. Although most extensively validated, a disadvantage of 18F-FDG is that the tracer is not specific. Recently, more specific tracers for plaque inflammation have been proposed [149–151], but these still need to be validated in larger studies. Alternatively, uptake of [1]^{8}F-sodium fluoride (NaF), a marker for active microcalcific processes, was reported at the site of carotid plaque rupture and larger uptake was demonstrated in symptomatic plaques [142,152,153]. The value of 18F–NaF for risk stratification is currently under investigation in an ongoing prospective multicenter trial (PREFFIR; unique identifier: NCT02278211).

5.2. Intravascular imaging platforms

The use of intravascular technologies for intraluminal imaging of carotid atherosclerosis is currently limited to highly selected cases and includes fiber-bundle angioscopy (FBA), IVUS, and optical coherence tomography (OCT). FBA was introduced in the early 1980s and initially applied to assess plaque disruption, luminal thrombus, and stent placement [154,155]. Despite the initial enthusiasm given the unprecedented images of the arterial lumen and surface, the poor image quality (<10,000 pixels even with FBA), the large size, and the excessive stiffness of the cameras significantly limited adoption [156]. Recent advances in photonics and optics allowed the development of Scanning

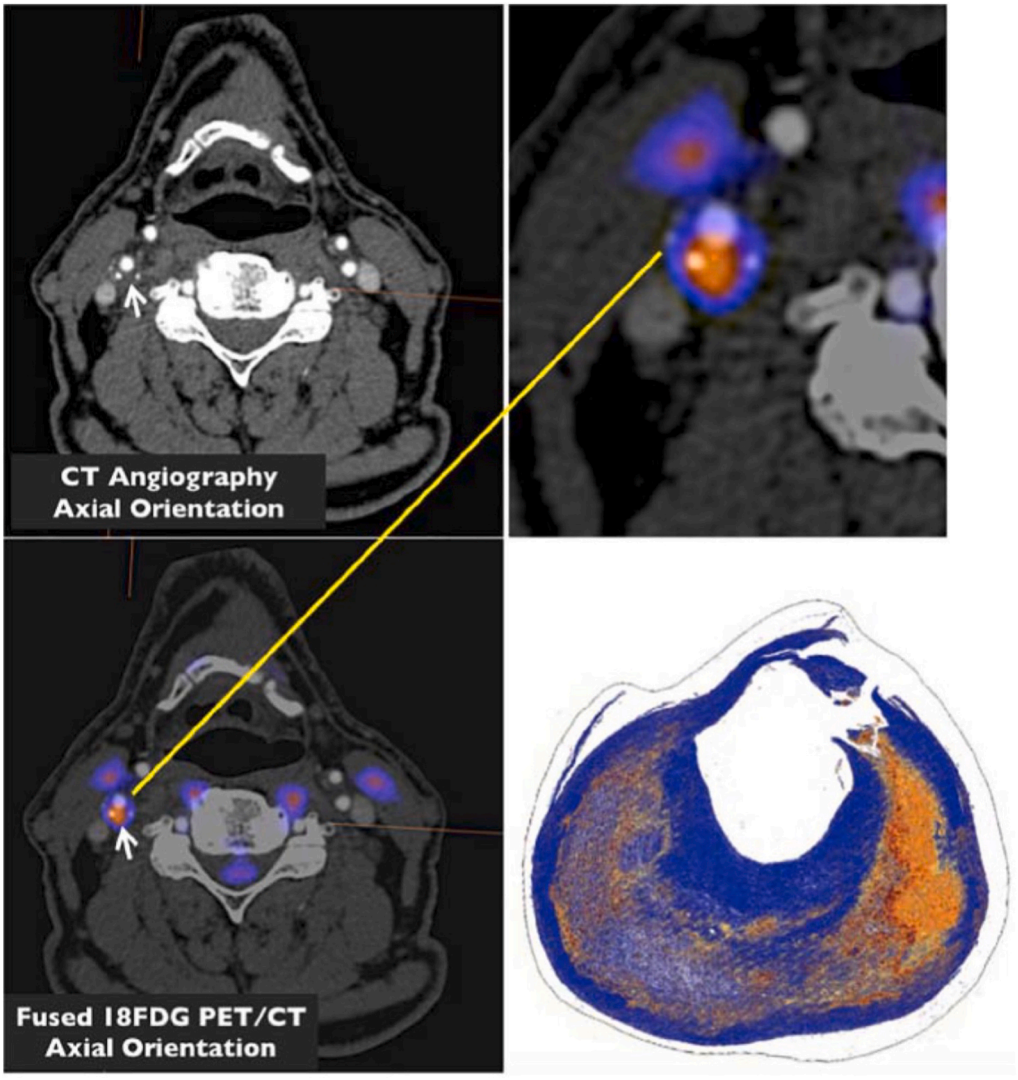

Fig. 3. Metabolic activity within atherosclerotic carotid plaque, imaged with [^{18}F]-fluorodeoxyglucose (^{18}FDG) hybrid PET/CT correlates with *ex-vivo* macrophage-specific CD68 CT angiography (axial plane) fused with [18F]-fluorodeoxyglucose PET in a patient with a symptomatic right internal carotid artery plaque (arrow).
From the fused PET/CT images, there are small regions of calcification with a narrowing of the right internal carotid artery. The tissue to blood ratio for maximum 18FDG uptake was 4.7. Following excision and advanced immunohistology, there is strong evidence for extensive CD68 staining (rust-stained regions), a marker of macrophage expression and direct inflammatory burden. Reproduced with permission of Elsevier from: Cocker MS, Spence JD, Hammond R et al. [^{18}F]-Fluorodeoxyglucose PET/CT imaging as a marker of carotid plaque inflammation: Comparison to immunohistology and relationship to acuity of events. International Journal of Cardiology. 2018; 271:378–386.

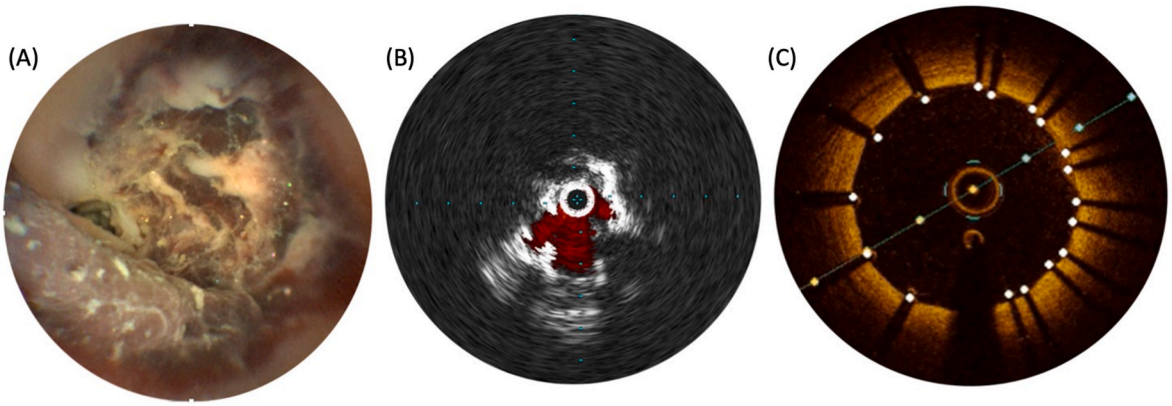

Fig. 4. (A) Laser-angioscopy showing an acutely disrupted plaque with red blood cell rich intraluminal thrombus resulting in critical stenosis; (B) IVUS images with doppler mode of a symptomatic calcified plaque causing severe irregular stenosis; (C) OCT images showing stent apposition in a carotid artery. (For interpretation of the references to color in this figure legend, the reader is referred to the Web version of this article.)

Fiber Angioscopy, a miniature laser-based platform capable of generating high resolution (~12 μm, or >250,000 pixels) structural, biochemical, and biological vascular videos in real time (Fig. 4A) [156, 157]. IVUS was introduced in the late 1980s and employs an intravascular piezoelectric transducer that creates waves that propagate through blood and tissue. IVUS generates cross-sectional imaging without the need of clearing the intravascular blood, but the resolution is poor (100–150 μm). IVUS has been clinically used to characterize the structure of carotid plaques by virtual histology, measure the degree of stenosis, and evaluate stent apposition and plaque protrusion in CAS

(Fig. 4B) [158–160]. OCT shines a near-infrared laser sideways and a small portion of this light (scattering) that reflects from sub-surface tissues is collected and processed by interferometry. Automated pull-back in a bloodless lumen results in cross-sectional images of arteries. The use of OCT in carotid arteries continues to be very limited in the evaluation of disrupted plaques, stent apposition, and tissue prolapse in CAS [161,162].

6. A look into the future

6.1. Artificial intelligence

As stroke is the second leading cause of global mortality, this demonstrated the need for improved tools in the management of occlusive vascular disease [163,164]. Patients with cardiovascular disease leading to stroke often require significant medical imaging in the acute, sub-acute, and chronic settings, using a range of imaging modalities. Vascular imaging is then used as a key source of information in the determination of appropriate clinical management. In the era of modern medicine, AI is an evolving field that is experiencing a steady development in vascular imaging [79,165,165,166]. In daily clinical practice, plaque assessment is performed through manual measurement of the degree of the stenosis and visual evaluation of plaque composition [6,167]. However, a manual evaluation has various limitations, including a long analysis time and is *highly* dependent on the operator. AI may evaluate carotid plaques with their vulnerable features to decide whether invasive investigation and treatment are necessary.

US is the modality of choice for initial evaluation and confirmation of carotid artery disease: characteristics of the carotid plaque in patients with carotid stenosis can identify those patients with relatively higher risk for stroke and help select patients who may benefit from intervention over medical treatment alone or vice versa. Symptomatic plaques tend to produce more tight stenosis, be more hypoechoic, have a large juxtaluminal black area close to the lumen without a visible echogenic cap, and discrete white hyperechoic areas compared with asymptomatic plaques [168,169]. Additional and more precise information can be derived from software implementations applied to ultrasound: 3D/4D, Intravascular Ultrasound (IVUS), CEUS, Sonoelastography, Vector Doppler, Grayscale Median (GSM), Radiofrequency, etc. The large datasets obtained from all these imaging sources are traditionally interpreted qualitatively by clinicians but are highly heterogeneous, varying due to differences in patient, imaging technology, and site scanning protocols. Current measurement methods are time-consuming and do not utilize the power of knowledge-based paradigms such as artificial intelligence (AI), a branch of computer science that includes machine learning (ML), deep learning (DL), and convolutional neural networks (CNNs) (Fig. 5). AI excels at automatically recognizing complex patterns and providing quantitative assessment for imaging data, showing high potential to assist physicians in acquiring more accurate and reproducible results [170,171]. Recently, a DL–based model was applied for carotid IMT and lumen measurement [172]. It was the first artificial intelligence-based approach to ultrasound-based carotid artery segmentation and carotid IMT (cWT þ CP) measurement that used 13 layers of convolution layers for feature extraction and three up-sample layers for segmentation. Deep learning resulted in a useful tool for carotid ultrasound-based characterization and classification of symptomatic and asymptomatic plaques in a more recent paper [173] where implementation with a supercomputer configuration was more precise and faster if compared with other AI systems. Further and more accurate measurements can be obtained when an AI-based model utilizing DL methodology is used on image patches rather than full-size images, mainly to have better local control in small regions rather than the whole image at once [170,172,174]. A new method consisting of a novel design of 10 types of solo deep learning (SDL) and hybrid deep learning (HDL) models focused on automated plaque segmentation in the internal carotid artery (ICA) has shown to be very useful in identifying plaques at risk of rupture: the system is very fast and precise (it takes <1 s per image) and it may therefore be practical to introduce such an AI-based system to detect rupture-prone plaques (or vulnrable plaque detection) [175].

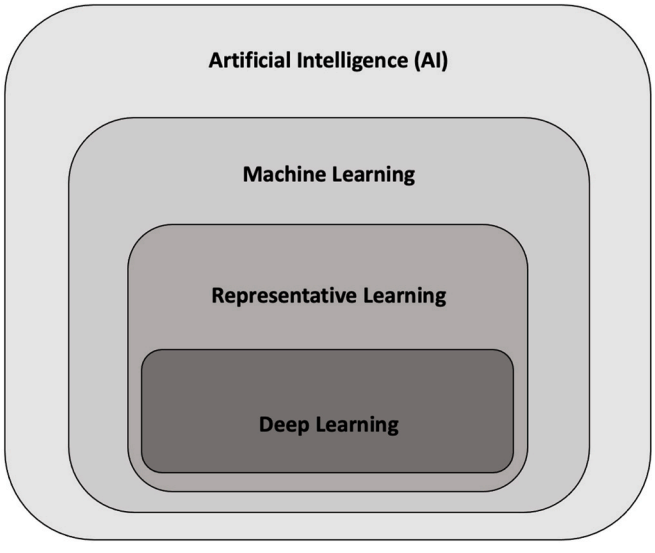

Fig. 5. Venn diagram illustrating the hierarchy of the artificial intelligence fields.

In addition to the improved ability to define so-called vulnerable plaques to enable the best therapeutic approach, AI has also proved to be useful for the evaluation of carotid artery stenting (CAS) prognosis and in the prediction of persistent hemodynamic depression after carotid angioplasty [176,177]. Of note, the application of AI to ultrasonographic diagnostics for better diagnosis and possibly new classification and standardization methods [178] requires close collaboration among computer scientists, clinical investigators, clinicians, and other users in order to identify the most relevant problems to be solved and the best approach and data sources to achieve this.

An AI-based approach has also proven its usefulness in CT. Acharya et al. investigated a supervised-learning model to classify carotid artery images into symptomatic and asymptomatic using a combination of local binary model and wavelet energy features [179]. The authors reported sensitivities, specificities, and accuracies of 0.88, 0.865, and 0.902, respectively [179]. Dos Santos et al. proposed a fully-automated, user-independent tool for the segmentation and analysis of atherosclerosis in the extracranial carotid arteries, reporting performance of 83% with accuracy, sensitivity, and specificity values of 71%, 83%, and 25%, respectively with an average difference between manual and automated analysis of 37% ($p = 027$) and an average analysis time of 1381 s per patient [180]. AI models have been also developed to simplify plaque characterization and predict histological plaque composition. Hanning et al. tested an ML-based analysis of admission non-contrast CT and CTA to predict thrombus composition with its fractions of fibrin and red blood cells [181]. This analysis included 112 patients who underwent thrombectomy due to carotid or middle cerebral artery occlusion, evaluating both vessel walls, thrombi, and peri-vascular tissue response. The ML-based algorithm demonstrated an AUC of 0.83 for differentiating thrombi with a high fraction of red blood cells (sensitivity and specificity of 77% and 74%, respectively) and an AUC of 0.84 for differentiating fibrin-rich thrombi (sensitivity and specificity of 81% and 73%, respectively) [181]. Another research investigated the ability of a DL-based model to identify symptomatic patients from asymptomatic patients and further discriminate between culprit and non-culprit carotid arteries in symptomatic patients [182]. This proposed model was 92% accurate in differentiating between symptomatic and asymptomatic patients, and 71% accurate in discriminating between culprit versus

non-culprit carotid arteries in symptomatic patients [182]. The relationship between carotid vessel image parameters and stroke risk was also investigated by Lal et al. using an artificial intelligence algorithm for risk stratification in carotid atherosclerosis incorporating a combination of carotid plaque geometry, plaque composition, patient demographics, and clinical information [183] AI is able to mesh a large amount of quantitative imaging data to clinical parameters, that may be a new frontier of AI in carotid plaque risk assessment improving diagnosis and decision-making in daily clinical practice.

AI is transforming most healthcare domains including carotid MRI. AI is increasingly used to reduce manual effort in carotid MRI measurements. Using a convolutional neural network (CNN) based algorithm called DeepMAD to separately segment the carotid lumen and outerwall contours on 2D T1w turbo spin-echo MRI, Wu et al. identified slices with atherosclerotic plaque [184]. Similarly, Samber et al. used two separate CNNs for lumen and outerwall segmentation of 2D T2w turbo spin echo MRI [185]. Chen et al. demonstrated a CNN algorithm called LATTE for segmentation [186] of the carotid vessel wall on 3D-MERGE [187] black-blood MRI using a polar transformation centered on the carotid after vessel identification. To make the segmentation robust to inter-scanner differences, domain adaptation for LATTE was developed and shown to improve the identification of advanced plaque [188]. Thus, quick, and automated screening for carotid plaque using 3D-MERGE is made possible by LATTE. The next frontier for carotid AI applications lies in plaque component segmentation. CNN-based segmentation of plaque components such as lipid-core, calcification, and intra-plaque hemorrhage on multi-contrast 2D MRI is able to better match the human expert's plaque component segmentation than non-CNN methods [189]. Zhang et al. compared several ML methods [190] for plaque component segmentation using a specific sequence called SNAP [191]. However, these methods are 2D MRI based and need to be modified for use with 3D carotid MRI. With future development, multi-contrast 3D plaque component segmentation may allow complete carotid plaque analysis and quantification with minimal user intervention thereby reducing clinician workloads and expanding the applications of carotid plaque MRI.

CNNs have also found applications in carotid MRA. Koktzoglou et al. demonstrated that non-contrast carotid MRI can be accelerated to below 3 min when combined with denoising of MRA using CNNs [192]. Ziegler et al. used the DeepMedic CNN on CE-MRA to segment the carotid artery into common, internal, and external carotid segments [193].

Information contained in the grey-scale differences among tissues is easily summarized by human-derived features. Radiomics can extract traditional grey scale level features from images to improve the diagnostic capabilities of carotid MRI. Zhang et al. showed that adding radiomic features of carotid plaque to traditional plaque features improved the model's ability to predict symptom status [190]. Application of such radiomics specific to the carotids requires segmentation of the carotid lumen and outer wall. Hence future combination of CNN based segmentation methods combined with radiomics may enable a comprehensive and automated analysis of both carotid MRI and other clinical variables to predict patient outcomes.

6.2. Radiomics

Since the 1990s, the improvement of resolution, which allows the identification of increasingly smaller lesions, and the availability of imaging modalities that provide morphological and functional information have introduced new scenarios and new diagnostic possibilities. The introduction of new imaging technologies such as ultrasound contrast agents, microvascular flow, elastography, and specific imaging processing techniques allows us to obtain improved morphological/functional quantitative information compared to those only derived from B-mode.

Precision medicine requires a clear understanding of each patient's heterogeneity and individual situation. Radiological images are often analysed and interpreted by the radiologist only qualitatively (visual evaluation). However, digital images are composed of individual pixels to which discrete brightness or colour values are assigned. They can be efficiently processed, objectively evaluated, and made available at many places at the same time by means of appropriate communication networks and protocols, such as PACS and DICOM protocols. In a digital image, a large amount of numerical data is not analysed by the radiologist. This "hidden" information can be used to create a "radiological plot", which can provide much more information on tissue than simple visual observations by providing objective data. The amount of data associated with digital imaging has increased and produced a large amount of electronic data ("Big Data"). In personalized and precision medicine, the data, analysed with complex mathematical algorithms and the use of artificial intelligence methods (Fig. 6) [194], can provide quantitative information on pathophysiological phenomena to improve diagnostic accuracy, prognostic, and predictive imaging capacity.

Artificial intelligence techniques consist of ML systems. The computer receives data and analyses the existing relationships using analysis systems that reproduce the functioning of the nervous system.

The term "radiomics" was defined by Lambin in 2012 [195] as the high-throughput extraction of image features from diagnostic images. The final product is a quantitative feature, measurable and minable, defined as an "imaging biomarker". Biomarkers are indicators of normal biological processes, pathological changes, or pharmaceutical responses to a therapeutic intervention [196,197]. Therefore, radiomics represents diagnostic and predictive support that, together with other clinical and genetic investigations, allows the formulation of personalized therapies and the evaluation of treatment response.

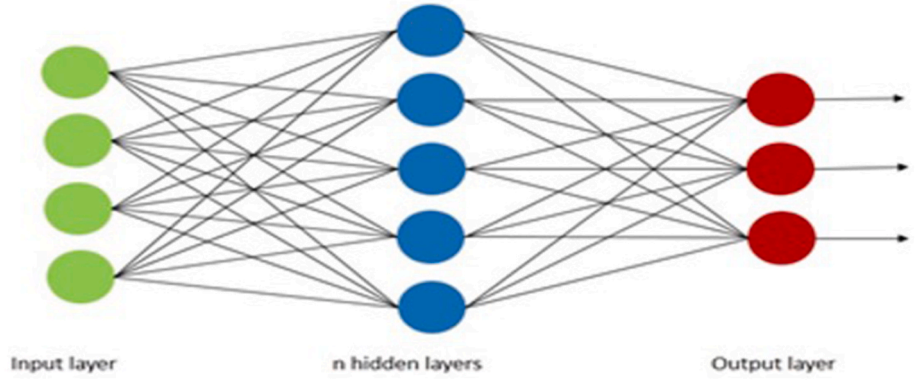

Fig. 6. Basic representation of an artificial neural network with neurons similar to those within a brain.
The left layer of the neural network is called the input layer and contains neurons that encode the values of the input pixels. The right most layer is called the output layer, which contains the output neurons. The middle contains the "n" number of hidden layers, which perform mathematical transformations of the data.

The radiomic data are extracted and processed with bioinformatics tools. They can be combined with other patient data (clinical, biohumoral, genetic) to develop models to improve diagnostic, prognostic, and predictive accuracies. Although radiomics is a natural extension of computer-aided diagnosis and detection (CAD) systems, it is significantly different from them. CAD systems are usually used for the detection or diagnosis of disease [198,199] and are directed towards delivering a single answer (presence or absence of disease). Radiomics is a process designed to extract a large number of quantitative features from digital images to generate pathophysiological hypotheses and provide information on the phenotype and microenvironment. These features, in conjunction with other information, can be correlated with clinical outcomes and used for clinical support. Radiomics has the potential to help with the diagnosis and visualization of lesion heterogeneity and may prove critical in the assessment of prognosis, prediction of response to treatment, and monitoring of disease status. The "omics" concept readily applies to quantitative tomographic imaging on multiple levels (one multi-layer or three-dimensional image from one patient may easily contain millions of voxels). Complex images with high-dimensional data are generated, corresponding to measurable biological characteristics.

Radiomics depicts the goal of precision medicine, in which stable, reproducible, and validated molecular biomarkers are used to predict "the right treatment for the right patient at the right time" [199,200].

The radiomic process can be divided into five phases [201]: 1) Image acquisition and reconstruction, 2) Segmentation and rendering, 3) Feature extraction and qualification, 4) Construction of a database, and 5) Modelling and validation.

The first step in the radiomics algorithm begins with the choice of an image acquisition protocol. This varies according to the clinical endpoint. However, image acquisition parameters, including radiation dose, scanning protocol, reconstruction algorithm, and slice thickness, vary widely in routine clinical practice. Therefore, a comparison of the features extracted from different methods of image acquisition is not possible. The radiomic features are generally sensitive to the acquisition protocols used, only some are stable despite the different image reconstruction settings. Significant efforts are required to identify univocal acquisition and reconstruction protocols and to match them between different scanners.

In most patients with carotid stenotic lesions, the volumes of interest can be identified. Furthermore, the subvolumes within atherosclerotic plaque, representative of plaque heterogeneity, can be analysed separately. With this approach, images with different acquisition parameters can be combined to yield regions with specific combinations of plaque features (cell density, necrotic core, hemorrhage, atherosclerotic fibrous cap, flow velocity, etc). Once the volumes of interest have been identified, the segmentation strategy must be chosen. This point is critical as the resulting feature values depend on the adopted segmentation methods, which should be stable and reproducible. Usually, manual segmentation by expert readers is considered the gold standard, but it is a time-consuming process with high inter-operator variability. Consequently, the best compromise has been identified in CAD systems that work semi-automatically, with subsequent human manual correction. The use of semi-automated methods has also paved the way for three-dimensional (3D) segmentation [200]. Volumetric segmentation allows a comprehensive view of the total lesion and burden, a more complete description of the shape, and a greater number of points included in the computation of statistical features, leading to more reliable results that do not suffer from sampling errors. Moreover, computer-aided approaches reduce the manual workload, allow fast, and reproducible volumetric segmentation in large cohorts of patients [200]. From the identified atherosclerotic plaque, multiple quantitative image features can be extracted, including features that describe the characteristics of the region under analysis, such as the histogram of signal intensity, shape, and texture, and descriptors of the position and its relationships with surrounding tissues. Features can be "semantic" or "agnostic". Semantic features are those commonly used by radiologists to describe regions of interest with qualitative descriptors such as size and shape. The agnostic features are mathematically extracted indicators that are generally not part of the traditional lexicon of radiologists and can be divided into first- and second-order statistical features [201]. The first-order features describe the intensity histogram by extracting features such as the maximum and average values in addition to the causality and asymmetry of the distribution and have the limitation of not providing information on the spatial relations between voxels. This information can be obtained from the statistical features of the second order, which, using texture analysis methods, describe the relations between the signal in a voxel and the signal in the neighbouring voxels. Overall, each category produces various quantitative parameters that reflect the specific aspects of a lesion. The power of a predictive classifier model is dependent on having sufficient data. A reasonable rule of thumb is that 10 samples (patients) are needed for each feature in a model based on binary classifiers. Furthermore, the best models are those that can accommodate additional clinical or genomic covariates. Radiomics can be performed with as few as 100 patients, although larger data sets provide more power. Radiomic and non-radiomic features should be combined with the prediction target to create a single dataset. After identification, features can be included or excluded from the model. Radiomic features that are well-correlated with routine clinical feature (such as symptoms) or features not correlated with the clinical end-point are excluded. A predictive model of clinical outcomes is constructed using the features extracted from the data set. Radiomics produces models for assessing the risk of stroke or for estimating the probability of patient survival. Independent validation datasets are needed to confirm the prognostic value of the same radiomic features. Model performance is measured using receiver operating characteristic (ROC) curve analysis, which measures accuracy throughout the range of possible model values and identifies the best cut-off value. The validation of a model must be accompanied by the verification of its reproducibility by repeating the analyses with the same procedures on different data sets. It is therefore important to have a comprehensive and detailed medical image database [202]. Multiple articles have focused on ML approaches for the role of image processing in thw prediction of cardiovascular event and demonstrated that can improve the accuracy of cardiovascular disease prediction and a better predictive capacity than some traditional risk scores [203–212].

7. Summary and conclusion

Ultrasonography is the first-line imaging modality for the evaluation of atherosclerotic carotid artery disease, as it is non-invasive, cost-effective, readily available, well-tolerated, and safe [213,214]. Anatomic information is provided with traditional B-mode (greyscale) ultrasound, while hemodynamic information is provided with color Doppler, power Doppler, and pulsed-wave Doppler technique [213,214].

The image quality provided by ultrasound can be enhanced by the use of a contrast agent [214]. The ultrasonographic contrast agent most often used is microbubbles of an inert gas stabilized by an outer shell consisting of phospholipids or albumin (e.g. sulfur hexafluoride or octafluoropropane) [214]. By use of CEUS, the carotid lumen and adventitia are enhanced, therefore making lumen irregularities more prominent and consequently more easily detectable [214]. CEUS compensates for the inherent limitations of Doppler techniques, such as a lower signal-to-noise ratio, lower sensitivity for slow flow, and technical artefacts such as Doppler angle dependence, aliasing, and overwriting artefacts [214]. Another use of CEUS is the so-called late-phase enhancement, where the ultrasound examination is performed 6 min after administration of the contrast material. Late-phase enhancement suggests an increased inflammatory cell load within the plaque, thus representing a possible marker for early plaque rupture [214].

Progression of total plaque area and total plaque volume with 3-D

ultrasound is a more accurate predictor of transient ischemic attacks, stroke, and death than the conventional color Doppler techniques [215]. Furthermore, 3-D ultrasound may evaluate carotid plaque surface and may identify carotid ulcers, which are associated with a higher incidence of long-term stroke or death [216,217].

By using multiple different high spatial resolution contrast weightings, MRI/MRA has the advantage of being able to measure all the hallmarks of carotid plaque vulnerability, namely carotid plaque burden, intraplaque hemorrhage, ulcerations, lipid-rich necrotic core, and thin or ruptured fibrous cap [218]. These imaging parameters could be included in a clinical risk prediction model to determine a more personalized stroke risk [218]. Advanced plaques characterized by a large lipid-rich necrotic core and thinning/rupture of the fibrous cap are associated with an increased risk of ischemic cerebrovascular events by 3-fold (95% CI: 1.51–5.95) and almost 6-fold (95% CI: 2.65–13.30), respectively [114]. Moreover, intraplaque hemorrhage on MRI is a strong and independent predictor for ipsilateral stroke (Hazard Ratio: 11.0; 95% CI: 4.8 to 25.1)[125]. MRI provides excellent soft-tissue contrast, no ionizing radiation and is not subject to technical challenges such as shadowing or blooming artefacts caused by calcium deposits [219]. MRI is well-validated, highly reproducible, and is recognized as the optimal imaging modality for non-invasive assessment of plaque composition for stroke prediction [219].

CTA is less operator-dependent than carotid ultrasound and is also more quickly performed and more widely available than MRI [220]. CTA evidence of a low-attenuation or "soft" plaque, an increased common carotid artery wall thickness, or plaque ulceration strongly correlates with a recent ipsilateral transient ischemic attack or stroke episode [220]. Evaluation of the presence of a soft, or calcified plaque, plaque ulceration or increased common carotid artery wall thickness can be easily performed with high reproducibility without requiring length of interpretation time or postprocessing software [220]. A recent study demonstrated that CTA may accurately identify specific markers which are more predictive of future stroke risk than the percentage of luminal stenosis, such as the presence of intraluminal thrombus, the maximum soft plaque thickness, and a thin adventitial calcification (the "rim sign") [221]. Thin peripheral calcification may be a marker of chronic adventitial inflammation and adventitial microvessel leakage has been implicated in carotid intraplaque hemorrhage [222]. These findings highlight the ability of CTA to identify plaque features that are strongly associated with cerebrovascular ischemia.

Identification of IPH using MRI, the presence of carotid plaque ulceration, plaque echolucency on Duplex ultrasound, and reduced cerebrovascular reserve are reliable predictors of future cerebrovascular events and may be used to identify high-risk patient subgroups and offer them a prophylactic carotid intervention [223]. The 2018 European Society for Vascular Surgery (ESVS) guidelines for the management of patients with carotid artery stenosis recommended that in "average surgical risk" patients with a 60–99% ACS, CEA should (Class IIa; Level of Evidence: B) or CAS may be considered (Class IIb; Level of Evidence: B) in the presence of one or more clinical/imaging characteristics that may be associated with an increased risk of late ipsilateral stroke, provided documented perioperative stroke/death rates are <3% and the patient's life expectancy is > 5 years [224]. These clinical/imaging characteristics included silent embolic infarcts on brain CTA/MRI, progression in the severity of ACS, a history of contralateral TIA/stroke, microemboli detection on TCD, the presence of IPH on MRI, plaque ulceration on 3D ultrasound or MRI, reduced cerebrovascular reserve, a large plaque area (>40 mm^2) on ultrasound longitudinal images and plaque echolucency as shown by a low GSM (<30) and presence of a large (>8 mm^2) juxtaluminal hypoechoic area after image normalization of Duplex ultrasound images [224]. A recent multinational survey of current practice in carotid imaging reported that the first exam used to evaluate carotid bifurcation disease in ACS patients was ultrasound in 88.8% of respondents, CTA in 7%, and MRA in 4.2% [225]. Nevertheless, it is worth mentioning that the percentage of luminal stenosis for which CEA or CAS was recommended for asymptomatic patients was reduced in the presence of imaging evidence of "vulnerable plaque features" by a third of study participants (n = 76 of 223 respondents; 34.2%) [225].

In conclusion, each imaging technique has its advantages and disadvantages when compared with the other available modalities. Issues like cost-effectiveness, availability, reproducibility of the results, and local expertise play an important role, but overall ultrasound should be considered as the initial imaging modality, followed by CTA or carotid MRA as second-line imaging options. The presence or lack of specific imaging parameters should aid physicians and surgeons in their decision-making and the selection of the optimal therapeutic approach for each patient, after also considering each patient's views, needs, and expectations [226]. There is an urgent need for modernized clinical prediction models that include imaging parameters on plaque vulnerability to determine a personalized stroke risk. Trials are warranted to investigate whether including these imaging parameters in clinical decision-making reduces stroke risk and improves the outcome of the patients.

CRediT authorship contribution statement

Luca Saba: Conceptualization, Methodology, Validation, Writing – review & editing. **Pier Luigi Antignani:** Conceptualization, Methodology, Validation, Writing – review & editing. **Ajay Gupta:** Conceptualization, Writing – original draft. **Riccardo Cau:** Conceptualization, Writing – original draft, Writing – review & editing. **Kosmas I. Paraskevas:** Methodology, Writing – original draft. **Pavel Poredos:** Methodology, Writing – original draft. **Bruce A. Wasserman:** Writing – original draft. **Hooman Kamel:** Writing – original draft. **Efthymios D. Avgerinos:** Writing – original draft. **Rodrigo Salgado:** Methodology, Writing – review & editing, Supervision. **Federico Caobelli:** Writing – original draft. **Leonardo Aluigi:** Methodology, Writing – original draft. **Luis Savastano:** Writing – original draft. **Martin Brown:** Writing – original draft. **Tom Hatsukami:** Methodology, Supervision. **Emad Hussein:** Validation, Supervision. **Jasjit S. Suri:** Conceptualization, Supervision. **Armado Mansilha:** Validation, Supervision. **Max Wintermark:** Writing – original draft. **Daniel Staub:** Conceptualization, Writing – review & editing. **Jose Fernandes Montequin:** Writing – original draft. **Ruben Tomas Toro Rodriguez:** Validation, Supervision. **Niranjan Balu:** Validation, Supervision. **Jan Pitha:** Writing, Validation, Supervision. **M. Eline Kooi:** Validation, Supervision. **Brajesh K. Lal:** Writing – original draft. **J. David Spence:** Writing – original draft. **Giuseppe Lanzino:** Conceptualization, Writing – review & editing. **Hugh Stephen Marcus:** Validation, Supervision. **Marcello Mancini:** Validation, Supervision. **Seemant Chaturvedi:** Writing – original draft. **Ales Blinc:** Conceptualization, Methodology, Validation.

Declaration of competing interest

The authors declare the following financial interests/personal relationships which may be considered as potential competing interests: Dr. Seemant Chaturvedi is on the executive committee of CREST 2 and ACT I and serves as an Associate Editor for *Stroke.* Dr. Luis Savastano is equity owner and CMO of VerAvanti Inc.

References

[1] D. Bos, D.H.K. van Dam-Nolen, A. Gupta, et al., Advances in multimodality carotid plaque imaging: AJR expert panel narrative review, AJR Am. J. Roentgenol. 217 (1) (2021) 16–26, https://doi.org/10.2214/AJR.20.24869.
[2] G. Chen, Y. Xue, J. Wei, Q. Duan, The undiagnosed potential clinically significant incidental findings of neck CTA: a large retrospective single-center study, Medicine (Baltimore) 99 (43) (2020), e22440, https://doi.org/10.1097/MD.0000000000022440.
[3] A.F. AbuRahma, E.D. Avgerinos, R.W. Chang, et al., Society for Vascular Surgery clinical practice guidelines for management of extracranial cerebrovascular

disease, J. Vasc. Surg. 75 (1S) (2022) 4S–22S, https://doi.org/10.1016/j.jvs.2021.04.073.
[4] K. Barlinn, H. Rickmann, H. Kitzler, et al., Validation of multiparametric ultrasonography criteria with digital subtraction angiography in carotid artery disease: a prospective multicenter study, Ultraschall der Med. 39 (5) (2018) 535–543, https://doi.org/10.1055/s-0043-119355.
[5] A.S. Jahromi, C.S. Cinà, Y. Liu, C.M. Clase, Sensitivity and specificity of color duplex ultrasound measurement in the estimation of internal carotid artery stenosis: a systematic review and meta-analysis, J. Vasc. Surg. 41 (6) (2005) 962–972, https://doi.org/10.1016/j.jvs.2005.02.044.
[6] V. Aboyans, J.-B. Ricco, M.-L.E.L. Bartelink, et al., ESC guidelines on the diagnosis and treatment of peripheral arterial diseases, in collaboration with the European society for vascular Surgery (ESVS): document covering atherosclerotic disease of extracranial carotid and vertebral, mesenteric, renal, Eur. Heart J. 39 (9) (2017) 763–816, https://doi.org/10.1093/eurheartj/ehx095, 2018.
[7] L.S. Hirt, Progression rate and ipsilateral neurological events in asymptomatic carotid stenosis, Stroke 45 (3) (2014) 702–706, https://doi.org/10.1161/STROKEAHA.111.613711.
[8] S.K. Kakkos, A.N. Nicolaides, I. Charalambous, et al., Predictors and clinical significance of progression or regression of asymptomatic carotid stenosis, J. Vasc. Surg. 59 (4) (2014) 956–967, https://doi.org/10.1016/j.jvs.2013.10.073.
[9] L.E. Mantella, K. Liblik, A.M. Johri, Vascular imaging of atherosclerosis: strengths and weaknesses, Atherosclerosis 319 (2021) 42–50, https://doi.org/10.1016/j.atherosclerosis.2020.12.021.
[10] K. Spanos, I. Tzorbatzoglou, P. Lazari, D. Maras, A.D. Giannoukas, Carotid artery plaque echomorphology and its association with histopathologic characteristics, J. Vasc. Surg. 68 (6) (2018) 1772–1780, https://doi.org/10.1016/j.jvs.2018.01.068.
[11] A. Gupta, K. Kesavabhotla, H. Baradaran, et al., Plaque echolucency and stroke risk in asymptomatic carotid stenosis: a systematic review and meta-analysis, Stroke 46 (1) (2015) 91–97, https://doi.org/10.1161/STROKEAHA.114.006091.
[12] A.N. Nicolaides, S.K. Kakkos, E. Kyriacou, et al., Asymptomatic internal carotid artery stenosis and cerebrovascular risk stratification, J. Vasc. Surg. 52 (6) (2010) 1485–1486, https://doi.org/10.1016/j.jvs.2010.07.021.
[13] M.K. Salem, M.J. Bown, R.D. Sayers, et al., Identification of patients with a histologically unstable carotid plaque using ultrasonic plaque image analysis, Eur. J. Vasc. Endovasc. Surg. Off. J. Eur. Soc. Vasc. Surg. 48 (2) (2014) 118–125, https://doi.org/10.1016/j.ejvs.2014.05.015.
[14] W. Brinjikji, A.A. Rabinstein, G. Lanzino, et al., Ultrasound characteristics of symptomatic carotid plaques: a systematic review and meta-analysis, Cerebrovasc. Dis. 40 (3–4) (2015) 165–174, https://doi.org/10.1159/000437339.
[15] A. van Engelen, T. Wannarong, G. Parraga, et al., Three-dimensional carotid ultrasound plaque texture predicts vascular events, Stroke 45 (9) (2014) 2695–2701, https://doi.org/10.1161/STROKEAHA.114.005752.
[16] J.D. Spence, Measurement of carotid plaque burden, Curr. Opin. Lipidol. 31 (5) (2020) 291–298, https://doi.org/10.1097/MOL.0000000000000706.
[17] H. Sillesen, S. Sartori, B. Sandholt, U. Baber, R. Mehran, V. Fuster, Carotid plaque thickness and carotid plaque burden predict future cardiovascular events in asymptomatic adult Americans, Eur. Heart J. Cardiovasc. Imaging 19 (9) (2018) 1042–1050, https://doi.org/10.1093/ehjci/jex239.
[18] P. Raggi, J.H. Stein, Carotid intima-media thickness should not be referred to as subclinical atherosclerosis: a recommended update to the editorial policy at Atherosclerosis, Atherosclerosis 312 (2020) 119–120, https://doi.org/10.1016/j.atherosclerosis.2020.09.015.
[19] J.H. Stein, C.E. Korcarz, R.T. Hurst, et al., Use of carotid ultrasound to identify subclinical vascular disease and evaluate cardiovascular disease risk: a consensus statement from the American Society of Echocardiography Carotid Intima-Media Thickness Task Force endorsed by the Society for Vascular Medicine, J. Am. Soc. Echocardiogr. 21 (2) (2008) 93–111.
[20] U. Baber, R. Mehran, S. Sartori, et al., Prevalence, impact, and predictive value of detecting subclinical coronary and carotid atherosclerosis in asymptomatic adults: the BioImage study, J. Am. Coll. Cardiol. 65 (11) (2015) 1065–1074, https://doi.org/10.1016/j.jacc.2015.01.017.
[21] E.F. Gudmundsson, G. Björnsdottir, S. Sigurdsson, et al., Carotid plaque is strongly associated with coronary artery calcium and predicts incident coronary heart disease in a population-based cohort, Atherosclerosis 346 (2022) 117–123, https://doi.org/10.1016/j.atherosclerosis.2022.01.018.
[22] U. Näslund, N. Ng, A. Lundgren, et al., Visualization of asymptomatic atherosclerotic disease for optimum cardiovascular prevention (VIPVIZA): a pragmatic, open-label, randomised controlled trial, Lancet (London, England) 393 (10167) (2019) 133–142, https://doi.org/10.1016/S0140-6736(18)32818-6.
[23] J.D. Spence, V. Coates, H. Li, et al., Effects of intensive medical therapy on microemboli and cardiovascular risk in asymptomatic carotid stenosis, Arch. Neurol. 67 (2) (2010) 180–186, https://doi.org/10.1001/archneurol.2009.289.
[24] H.A. Pérez, A.O. Adeoye, L. Aballay, L.A. Armando, N.H. García, An intensive follow-up in subjects with cardiometabolic high-risk, Nutr. Metabol. Cardiovasc. Dis. 31 (10) (2021) 2860–2869, https://doi.org/10.1016/j.numecd.2021.06.011.
[25] A. Adams, W. Bojara, M. Romanens, Effect of statin treatment in patients with advanced carotid atherosclerosis: an observational outcome study, Cardiol. Res. 12 (6) (2021) 335–339, https://doi.org/10.14740/cr1318.
[26] J.D. Spence, D.G. Hackam, Treating arteries instead of risk factors: a paradigm change in management of atherosclerosis, Stroke 41 (6) (2010) 1193–1199, https://doi.org/10.1161/STROKEAHA.110.577973.
[27] J.D. Spence, Genetics of atherosclerosis: the power of plaque burden and progression: invited commentary on Dong C, Beecham A, Wang L, Blanton SH, Rundek T, Sacco RL. Follow-Up association study of linkage regions reveals multiple candidate genes for carotid plaque i, Atherosclerosis 223 (1) (2012) 98–101, https://doi.org/10.1016/j.atherosclerosis.2012.03.040.
[28] C. Bogiatzi, G. Gloor, E. Allen-Vercoe, et al., Metabolic products of the intestinal microbiome and extremes of atherosclerosis, Atherosclerosis 273 (2018) 91–97, https://doi.org/10.1016/j.atherosclerosis.2018.04.015.
[29] C.D. Ainsworth, C.C. Blake, A. Tamayo, V. Beletsky, A. Fenster, J.D. Spence, 3D ultrasound measurement of change in carotid plaque volume: a tool for rapid evaluation of new therapies, Stroke 36 (9) (2005) 1904–1909, https://doi.org/10.1161/01.STR.0000178543.19433.20.
[30] R. Zhou, A. Fenster, Y. Xia, J.D. Spence, M. Ding, Deep learning-based carotid media-adventitia and lumen-intima boundary segmentation from three-dimensional ultrasound images, Med. Phys. 46 (7) (2019) 3180–3193, https://doi.org/10.1002/mp.13581.
[31] R. Zhou, F. Guo, M.R. Azarpazhooh, et al., A voxel-based fully convolution network and continuous max-flow for carotid vessel-wall-volume segmentation from 3D ultrasound images, IEEE Trans. Med. Imag. 39 (9) (2020) 2844–2855, https://doi.org/10.1109/TMI.2020.2975231.
[32] R. Zhou, F. Guo, M.R. Azarpazhooh, et al., Deep learning-based measurement of total plaque area in B-mode ultrasound images, IEEE J. Biomed. Health Inf. 25 (8) (2021) 2967–2977, https://doi.org/10.1109/JBHI.2021.3060163.
[33] D. Russell, K.P. Madden, W.M. Clark, P.M. Sandset, J.A. Zivin, Detection of arterial emboli using Doppler ultrasound in rabbits, Stroke 22 (2) (1991) 253–258, https://doi.org/10.1161/01.str.22.2.253.
[34] E.B. Ringelstein, D.W. Droste, V.L. Babikian, et al., Consensus on microembolus detection by TCD. International consensus group on microembolus detection, Stroke 29 (3) (1998) 725–729, https://doi.org/10.1161/01.str.29.3.725.
[35] Z. Kaposzta, E. Young, P.M. Bath, H.S. Markus, Clinical application of asymptomatic embolic signal detection in acute stroke: a prospective study, Stroke 30 (9) (1999) 1814–1818, https://doi.org/10.1161/01.str.30.9.1814.
[36] J. Molloy, H.S. Markus, Asymptomatic embolization predicts stroke and TIA risk in patients with carotid artery stenosis, Stroke 30 (7) (1999) 1440–1443, https://doi.org/10.1161/01.str.30.7.1440.
[37] M. Sitzer, W. Müller, M. Siebler, et al., Plaque ulceration and lumen thrombus are the main sources of cerebral microemboli in high-grade internal carotid artery stenosis, Stroke 26 (7) (1995) 1231–1233, https://doi.org/10.1161/01.str.26.7.1231.
[38] H.S. Markus, A. King, M. Shipley, et al., Asymptomatic embolisation for prediction of stroke in the Asymptomatic Carotid Emboli Study (ACES): a prospective observational study, Lancet Neurol. 9 (7) (2010) 663–671, https://doi.org/10.1016/S1474-4422(10)70120-4.
[39] A. King, H.S. Markus, Doppler embolic signals in cerebrovascular disease and prediction of stroke risk: a systematic review and meta-analysis, Stroke 40 (12) (2009) 3711–3717, https://doi.org/10.1161/STROKEAHA.109.563056.
[40] H.S. Markus, D.W. Droste, M. Kaps, et al., Dual antiplatelet therapy with clopidogrel and aspirin in symptomatic carotid stenosis evaluated using Doppler embolic signal detection: the Clopidogrel and Aspirin for Reduction of Emboli in Symptomatic Carotid Stenosis (CARESS) trial, Circulation 111 (17) (2005) 2233–2240, https://doi.org/10.1161/01.CIR.0000163561.90680.1C.
[41] L.M.J. Best, A.C. Webb, K.S. Gurusamy, S.F. Cheng, T. Richards, Transcranial Doppler ultrasound detection of microemboli as a predictor of cerebral events in patients with symptomatic and asymptomatic carotid disease: a systematic review and meta-analysis, Eur. J. Vasc. Endovasc. Surg. Off. J. Eur. Soc. Vasc. Surg. 52 (5) (2016) 565–580, https://doi.org/10.1016/j.ejvs.2016.05.019.
[42] R. Topakian, A. King, S.U. Kwon, A. Schaafsma, M. Shipley, H.S. Markus, Ultrasonic plaque echolucency and emboli signals predict stroke in asymptomatic carotid stenosis, Neurology 77 (8) (2011) 751–758, https://doi.org/10.1212/WNL.0b013e31822b00a6.
[43] M. Goertler, M. Baeumer, R. Kross, et al., Rapid decline of cerebral microemboli of arterial origin after intravenous acetylsalicylic acid, Stroke 30 (1) (1999) 66–69, https://doi.org/10.1161/01.str.30.1.66.
[44] S.C. Johnston, J.D. Easton, M. Farrant, et al., Clopidogrel and aspirin in acute ischemic stroke and high-risk TIA, N. Engl. J. Med. 379 (3) (2018) 215–225, https://doi.org/10.1056/NEJMoa1800410.
[45] A. Safouris, C. Krogias, V.K. Sharma, et al., Statin pretreatment and microembolic signals in large artery atherosclerosis, Arterioscler. Thromb. Vasc. Biol. 37 (7) (2017) 1415–1422, https://doi.org/10.1161/ATVBAHA.117.309292.
[46] Y. Wang, Y. Wang, X. Zhao, et al., Clopidogrel with aspirin in acute minor stroke or transient ischemic attack, N. Engl. J. Med. 369 (1) (2013) 11–19, https://doi.org/10.1056/NEJMoa1215340.
[47] D. Staub, S. Partovi, S. Imfeld, et al., Novel applications of contrast-enhanced ultrasound imaging in vascular medicine, Vasa 42 (1) (2013) 17–31, https://doi.org/10.1024/0301-1526/a000244.
[48] D. Staub, A.F.L. Schinkel, B. Coll, et al., Contrast-enhanced ultrasound imaging of the vasa vasorum: from early atherosclerosis to the identification of unstable plaques, JACC Cardiovasc. Imag. 3 (7) (2010) 761–771, https://doi.org/10.1016/j.jcmg.2010.02.007.
[49] V. Rafailidis, X. Li, P.S. Sidhu, S. Partovi, D. Staub, Contrast imaging ultrasound for the detection and characterization of carotid vulnerable plaque, Cardiovasc. Diagn. Ther. 10 (4) (2020) 965–981, https://doi.org/10.21037/cdt.2020.01.08.
[50] A.F.L. Schinkel, J.G. Bosch, D. Staub, D. Adam, S.B. Feinstein, Contrast-enhanced ultrasound to assess carotid intraplaque neovascularization, Ultrasound Med. Biol. 46 (3) (2020) 466–478, https://doi.org/10.1016/j.ultrasmedbio.2019.10.020.

[51] V. Rafailidis, I. Chryssogonidis, C. Xerras, et al., A comparative study of color Doppler imaging and contrast-enhanced ultrasound for the detection of ulceration in patients with carotid atherosclerotic disease, Eur. Radiol. 29 (4) (2019) 2137–2145, https://doi.org/10.1007/s00330-018-5773-8.
[52] V. Rafailidis, I. Chryssogonidis, C. Xerras, et al., An ultrasonographic multiparametric carotid plaque risk index associated with cerebrovascular symptomatology: a study comparing color Doppler imaging and contrast-enhanced ultrasonography, AJNR Am. J. Neuroradiol. 40 (6) (2019) 1022–1028, https://doi.org/10.3174/ajnr.A6056.
[53] D. Staub, S. Partovi, A.F.L. Schinkel, et al., Correlation of carotid artery atherosclerotic lesion echogenicity and severity at standard US with intraplaque neovascularization detected at contrast-enhanced US, Radiology 258 (2) (2011) 618–626, https://doi.org/10.1148/radiol.10101008.
[54] D. Staub, M.B. Patel, A. Tibrewala, et al., Vasa vasorum and plaque neovascularization on contrast-enhanced carotid ultrasound imaging correlates with cardiovascular disease and past cardiovascular events, Stroke 41 (1) (2010) 41–47, https://doi.org/10.1161/STROKEAHA.109.560342.
[55] C. Li, W. He, D. Guo, et al., Quantification of carotid plaque neovascularization using contrast-enhanced ultrasound with histopathologic validation, Ultrasound Med. Biol. 40 (8) (2014) 1827–1833, https://doi.org/10.1016/j.ultrasmedbio.2014.02.010.
[56] S.C.H. van den Oord, Z. Akkus, J.G. Bosch, et al., Quantitative contrast-enhanced ultrasound of intraplaque neovascularization in patients with carotid atherosclerosis, Ultraschall der Med. 36 (2) (2015) 154–161, https://doi.org/10.1055/s-0034-1366410.
[57] M. Kaspar, I. Baumgartner, D. Staub, H. Drexel, C. Thalhammer, Non-invasive ultrasound-based imaging of atherosclerosis, Vasa 48 (2) (2019) 126–133, https://doi.org/10.1024/0301-1526/a000747.
[58] S. Coli, M. Magnoni, G. Sangiorgi, et al., Contrast-enhanced ultrasound imaging of intraplaque neovascularization in carotid arteries: correlation with histology and plaque echogenicity, J. Am. Coll. Cardiol. 52 (3) (2008) 223–230, https://doi.org/10.1016/j.jacc.2008.02.082.
[59] A. Hoogi, D. Adam, A. Hoffman, H. Kerner, S. Reisner, D. Gaitini, Carotid plaque vulnerability: quantification of neovascularization on contrast-enhanced ultrasound with histopathologic correlation, AJR Am. J. Roentgenol. 196 (2) (2011) 431–436, https://doi.org/10.2214/AJR.10.4522.
[60] C. Schmidt, T. Fischer, R.-I. Rückert, et al., Identification of neovascularization by contrast-enhanced ultrasound to detect unstable carotid stenosis, PLoS One 12 (4) (2017), e0175331, https://doi.org/10.1371/journal.pone.0175331.
[61] H. Yan, X. Wu, Y. He, D. Staub, X. Wen, Y. Luo, Carotid intraplaque neovascularization on contrast-enhanced ultrasound correlates with cardiovascular events and poor prognosis: a systematic review and meta-analysis, Ultrasound Med. Biol. 47 (2) (2021) 167–176, https://doi.org/10.1016/j.ultrasmedbio.2020.10.013.
[62] Z. Li, X. Xu, L. Ren, et al., Prospective study about the relationship between CEUS of carotid intraplaque neovascularization and ischemic stroke in TIA patients, Front. Pharmacol. 10 (2019) 672, https://doi.org/10.3389/fphar.2019.00672.
[63] L. Cui, Y. Xing, Y. Zhou, et al., Carotid intraplaque neovascularisation as a predictive factor for future vascular events in patients with mild and moderate carotid stenosis: an observational prospective study, Ther. Adv. Neurol. Disord. 14 (2021), 17562864211023992, https://doi.org/10.1177/17562864211023992.
[64] L.E. Mantella, K.N. Colledanchise, M.-F. Hétu, S.B. Feinstein, J. Abunassar, A. M. Johri, Carotid intraplaque neovascularization predicts coronary artery disease and cardiovascular events, Eur. Heart J. Cardiovasc. Imaging 20 (11) (2019) 1239–1247, https://doi.org/10.1093/ehjci/jez070.
[65] M. Magnoni, E. Ammirati, F. Moroni, G.D. Norata, P.G. Camici, Impact of cardiovascular risk factors and pharmacologic treatments on carotid intraplaque neovascularization detected by contrast-enhanced ultrasound, J. Am. Soc. Echocardiogr. Off. Publ. Am. Soc. Echocardiogr. 32 (1) (2019) 113–120, https://doi.org/10.1016/j.echo.2018.09.001, e6.
[66] G.B. Anderson, R. Ashforth, D.E. Steinke, R. Ferdinandy, J.M. Findlay, CT angiography for the detection and characterization of carotid artery bifurcation disease, Stroke 31 (9) (2000) 2168–2174, https://doi.org/10.1161/01.str.31.9.2168.
[67] X. Leclerc, O. Godefroy, J.P. Pruvo, D. Leys, Computed tomographic angiography for the evaluation of carotid artery stenosis, Stroke 26 (9) (1995) 1577–1581, https://doi.org/10.1161/01.str.26.9.1577.
[68] B. Randoux, B. Marro, F. Koskas, et al., Carotid artery stenosis: prospective comparison of CT, three-dimensional gadolinium-enhanced MR, and conventional angiography, Radiology 220 (1) (2001) 179–185, https://doi.org/10.1148/radiology.220.1.r01jl35179.
[69] C.-J. Chen, T.-H. Lee, H.-L. Hsu, et al., Multi-Slice CT angiography in diagnosing total versus near occlusions of the internal carotid artery: comparison with catheter angiography, Stroke 35 (1) (2004) 83–85, https://doi.org/10.1161/01.STR.0000106139.38566.B2.
[70] M.J.W. Koelemay, P.J. Nederkoorn, J.B. Reitsma, C.B. Majoie, Systematic review of computed tomographic angiography for assessment of carotid artery disease, Stroke 35 (10) (2004) 2306–2312, https://doi.org/10.1161/01.STR.0000141426.63959.cc.
[71] C. Porsche, L. Walker, D. Mendelow, D. Birchall, Evaluation of cross-sectional luminal morphology in carotid atherosclerotic disease by use of spiral CT angiography, Stroke 32 (11) (2001) 2511–2515, https://doi.org/10.1161/hs1101.098153.
[72] J.E. Dix, A.J. Evans, D.F. Kallmes, A.H. Sobel, C.D. Phillips, Accuracy and precision of CT angiography in a model of carotid artery bifurcation stenosis, AJNR Am. J. Neuroradiol. 18 (3) (1997) 409–415.
[73] A. Napoli, D. Fleischmann, F.P. Chan, et al., Computed tomography angiography: state-of-the-art imaging using multidetector-row technology, J. Comput. Assist. Tomogr. 28 (Suppl 1) (2004) S32–45, https://doi.org/10.1097/01.rct.0000120859.80935.10.
[74] M. Prokop, A. Waaijer, S. Kreuzer, CT angiography ofthe carotid arteries, JBR-BTR organe la Soc R belge Radiol = orgaan van K Belgische Ver voor Radiol. 87 (1) (2004) 23–29.
[75] E.S. Bartlett, T.D. Walters, S.P. Symons, A.J. Fox, Quantification of carotid stenosis on CT angiography, AJNR Am. J. Neuroradiol. 27 (1) (2006) 13–19.
[76] L. Saba, T. Saam, H.R. Jäger, et al., Imaging biomarkers of vulnerable carotid plaques for stroke risk prediction and their potential clinical implications, Lancet Neurol. 4422 (19) (2019) 1–14, https://doi.org/10.1016/S1474-4422(19)30035-3.
[77] L. Saba, M. Anzidei, B.C. Marincola, et al., Imaging of the carotid artery vulnerable plaque, Cardiovasc. Intervent. Radiol. 37 (3) (2014) 572–585, https://doi.org/10.1007/s00270-013-0711-2.
[78] F. Cademartiri, A. Balestrieri, R. Cau, et al., Insight from imaging on plaque vulnerability: similarities and differences between coronary and carotid arteries—implications for systemic therapies, Cardiovasc. Diagn. Ther. 10 (4) (2020) 1150–1162, https://doi.org/10.21037/cdt-20-528.
[79] R. Cau, A. Flanders, L. Mannelli, et al., Artificial intelligence in computed tomography plaque characterization: a review, Eur. J. Radiol. (2021), 109767, https://doi.org/10.1016/j.ejrad.2021.109767. Published online.
[80] J.-B. Michel, R. Virmani, E. Arbustini, G. Pasterkamp, Intraplaque haemorrhages as the trigger of plaque vulnerability, Eur. Heart J. 32 (16) (2011) 1977–1985, https://doi.org/10.1093/eurheartj/ehr054, 1985a, 1985b, 1985c.
[81] T. Saam, H. Hetterich, V. Hoffmann, et al., Meta-analysis and systematic review of the predictive value of carotid plaque hemorrhage on cerebrovascular events by magnetic resonance imaging, J. Am. Coll. Cardiol. 62 (12) (2013) 1081–1091, https://doi.org/10.1016/j.jacc.2013.06.015.
[82] N. Singh, A.R. Moody, V. Panzov, D.J. Gladstone, Carotid intraplaque hemorrhage in patients with embolic stroke of undetermined source, J. Stroke Cerebrovasc. Dis. Off. J. Natl. Stroke Assoc. 27 (7) (2018) 1956–1959, https://doi.org/10.1016/j.jstrokecerebrovasdis.2018.02.042.
[83] L. Saba, M. Francone, P.P. Bassareo, et al., CT attenuation analysis of carotid intraplaque hemorrhage, AJNR Am. J. Neuroradiol. 39 (1) (2018) 131–137, https://doi.org/10.3174/ajnr.A5461.
[84] L.B. Eisenmenger, B.W. Aldred, S.-E. Kim, et al., Prediction of carotid intraplaque hemorrhage using adventitial calcification and plaque thickness on CTA, AJNR Am. J. Neuroradiol. 37 (8) (2016) 1496–1503, https://doi.org/10.3174/ajnr.A4765.
[85] J. Cai, T.S. Hatsukami, M.S. Ferguson, et al., In vivo quantitative measurement of intact fibrous cap and lipid-rich necrotic core size in atherosclerotic carotid plaque: comparison of high-resolution, contrast-enhanced magnetic resonance imaging and histology, Circulation 112 (22) (2005) 3437–3444, https://doi.org/10.1161/CIRCULATIONAHA.104.528174.
[86] R.C. Cury, S.L. Houser, K.L. Furie, et al., Vulnerable plaque detection by 3.0 tesla magnetic resonance imaging, Invest. Radiol. 41 (2) (2006) 112–115, https://doi.org/10.1097/01.rli.0000186419.55504.30.
[87] D. Xu, D.S. Hippe, H.R. Underhill, et al., Prediction of high-risk plaque development and plaque progression with the carotid atherosclerosis score, JACC Cardiovasc. Imag. 7 (4) (2014) 366–373, https://doi.org/10.1016/j.jcmg.2013.09.022.
[88] L. Saba, C. Yuan, T.S. Hatsukami, et al., Carotid artery wall imaging: perspective and guidelines from the ASNR vessel wall imaging study group and expert consensus recommendations of the American society of neuroradiology, Am. J. Neuroradiol. 39 (2) (2018), https://doi.org/10.3174/ajnr.A5488.
[89] L. Saba, N. Agarwal, R. Cau, et al., Review of imaging biomarkers for the vulnerable carotid plaque, JVS Vasc. Sci. 2 (2021) 149–158, https://doi.org/10.1016/j.jvssci.2021.03.001. Published online.
[90] G. Cerrone, D. Fanni, M.L. Lai, et al., Plasma cells in the carotid plaque: occurrence and significance, Eur. Rev. Med. Pharmacol. Sci. 25 (11) (2021) 4064–4068, https://doi.org/10.26355/eurrev_202106_26047.
[91] M.J. McCarthy, I.M. Loftus, M.M. Thompson, et al., Angiogenesis and the atherosclerotic carotid plaque: an association between symptomatology and plaque morphology, J. Vasc. Surg. 30 (2) (1999) 261–268, https://doi.org/10.1016/s0741-5214(99)70136-9.
[92] L. Saba, M.L. Lai, R. Montisci, et al., Association between carotid plaque enhancement shown by multidetector CT angiography and histologically validated microvessel density, Eur. Radiol. 22 (10) (2012) 2237–2245, https://doi.org/10.1007/s00330-012-2467-5.
[93] H.J. Barnett, D.W. Taylor, M. Eliasziw, et al., Benefit of carotid endarterectomy in patients with symptomatic moderate or severe stenosis. North American Symptomatic Carotid Endarterectomy Trial Collaborators, N. Engl. J. Med. 339 (20) (1998) 1415–1425, https://doi.org/10.1056/NEJM199811123392002.
[94] L. Saba, G. Caddeo, R. Sanfilippo, R. Montisci, G. Mallarini, CT and ultrasound in the study of ulcerated carotid plaque compared with surgical results: potentialities and advantages of multidetector row CT angiography, AJNR Am. J. Neuroradiol. 28 (6) (2007) 1061–1066, https://doi.org/10.3174/ajnr.A0486.
[95] L. Saba, G. Caddeo, R. Sanfilippo, R. Montisci, G. Mallarini, Efficacy and sensitivity of axial scans and different reconstruction methods in the study of the ulcerated carotid plaque using multidetector-row CT angiography: comparison with surgical results, AJNR Am. J. Neuroradiol. 28 (4) (2007) 716–723.

[96] S. Rozie, T.T. de Weert, C. de Monyé, et al., Atherosclerotic plaque volume and composition in symptomatic carotid arteries assessed with multidetector CT angiography; relationship with severity of stenosis and cardiovascular risk factors, Eur. Radiol. 19 (9) (2009) 2294–2301, https://doi.org/10.1007/s00330-009-1394-6.
[97] R. Pini, G. Faggioli, S. Fittipaldi, et al., Relationship between calcification and vulnerability of the carotid plaques, Ann. Vasc. Surg. (2017) 336–342, https://doi.org/10.1016/j.avsg.2017.04.017, 44(May).
[98] J. Yang, X. Pan, B. Zhang, et al., Superficial and multiple calcifications and ulceration associate with intraplaque hemorrhage in the carotid atherosclerotic plaque, Eur. Radiol. 28 (12) (2018) 4968–4977, https://doi.org/10.1007/s00330-018-5535-7.
[99] L.B. Eisenmenger, B.W. Aldred, S.E. Kim, et al., Prediction of carotid intraplaque hemorrhage using adventitial calcification and plaque thickness on CTA, Am. J. Neuroradiol. 37 (8) (2016) 1496–1503, https://doi.org/10.3174/ajnr.A4765.
[100] L. Saba, H. Chen, R. Cau, et al., Impact analysis of different CT configurations of carotid artery plaque calcifications on cerebrovascular events, AJNR Am. J. Neuroradiol. 43 (2) (2022) 272–279, https://doi.org/10.3174/ajnr.A7401.
[101] L. Saba, V. Nardi, R. Cau, et al., Carotid artery plaque calcifications: lessons from histopathology to diagnostic imaging, Stroke 53 (1) (2022) 290–297, https://doi.org/10.1161/STROKEAHA.121.035692.
[102] R.W. Baumgartner, M. Arnold, I. Baumgartner, et al., Carotid dissection with and without ischemic events: local symptoms and cerebral artery findings, Neurology 57 (5) (2001) 827–832.
[103] R. Hakimi, S. Sivakumar, Imaging of carotid dissection, Curr. Pain Headache Rep. 23 (1) (2019) 1–7.
[104] D. Kadian-Dodov, H.L. Gornik, X. Gu, et al., Dissection and aneurysm in patients with fibromuscular dysplasia: findings from the U.S. Registry for FMD, J. Am. Coll. Cardiol. 68 (2) (2016) 176–185, https://doi.org/10.1016/j.jacc.2016.04.044.
[105] T.P. Madaelil, J.A. Grossberg, R.G. Nogueira, et al., Multimodality imaging in carotid web, Front. Neurol. 10 (2019). https://www.frontiersin.org/article/10.3389/fneur.2019.00220.
[106] K. Wojcik, J. Milburn, G. Vidal, A. Steven, Carotid webs: radiographic appearance and significance, Ochsner J. 18 (2) (2018) 115–120, https://doi.org/10.31486/toj.18.0001.
[107] S. Priyadarshni, A. Neralla, J. Reimon, S. Smithson, Carotid webs: an unusual presentation of fibromuscular dysplasia, Cureus 12 (8) (2020), https://doi.org/10.7759/cureus.9549 e9549-e9549.
[108] A.A.K. Abdel Razek, H. Alvarez, S. Bagg, S. Refaat, M. Castillo, Imaging spectrum of CNS vasculitis, Radiographics 34 (4) (2014) 873–894, https://doi.org/10.1148/rg.344135028.
[109] J.C. Jennette, R.J. Falk, P.A. Bacon, et al., Revised international Chapel Hill consensus conference nomenclature of vasculitides, Arthritis Rheum. 65 (1) (2012) 1–11, https://doi.org/10.1002/art.37715, 2013.
[110] MRC European Carotid Surgery Trial: interim results for symptomatic patients with severe (70-99%) or with mild (0-29%) carotid stenosis. European Carotid Surgery Trialists' Collaborative Group, Lancet (London, England) 337 (8752) (1991) 1235–1243.
[111] M.D. Walker, J.R. Marler, M. Goldstein, et al., Endarterectomy for asymptomatic carotid artery stenosis, JAMA 273 (18) (1995) 1421–1428, https://doi.org/10.1001/jama.1995.03520420037035.
[112] A. Halliday, M. Harrison, E. Hayter, et al., 10-year stroke prevention after successful carotid endarterectomy for asymptomatic stenosis (ACST-1): a multicentre randomised trial, Lancet (London, England) 376 (9746) (2010) 1074–1084, https://doi.org/10.1016/S0140-6736(10)61197-X.
[113] E. Messas, G. Goudot, A. Halliday, et al., Management of carotid stenosis for primary and secondary prevention of stroke: state-of-the-art 2020: a critical review, Eur. Heart J. Suppl. 22 (Suppl M) (2020) M35–M42, https://doi.org/10.1093/eurheartj/suaa162.
[114] A. Gupta, H. Baradaran, A.D. Schweitzer, et al., Carotid plaque MRI and stroke risk: a systematic review and meta-analysis, Stroke 44 (11) (2013) 3071–3077, https://doi.org/10.1161/STROKEAHA.113.002551.
[115] B.A. Wasserman, Advanced contrast-enhanced MRI for looking beyond the lumen to predict stroke, Stroke 41 (10_suppl_1) (2010) S12–S16, https://doi.org/10.1161/STROKEAHA.110.596288.
[116] B.A. Wasserman, R.J. Wityk, H.H. Trout, R. Virmani, Low-grade carotid stenosis: looking beyond the lumen with MRI, Stroke 36 (11) (2005) 2504–2513, https://doi.org/10.1161/01.STR.0000185726.83152.00.
[117] D.H. O'Leary, J.F. Polak, R.A. Kronmal, et al., Distribution and correlates of sonographically detected carotid artery disease in the cardiovascular Health study. The CHS collaborative research group, Stroke 23 (12) (1992) 1752–1760, https://doi.org/10.1161/01.str.23.12.1752.
[118] B.C. Astor, A.R. Sharrett, J. Coresh, L.E. Chambless, B.A. Wasserman, Remodeling of carotid arteries detected with MR imaging: atherosclerosis risk in communities carotid MRI study, Radiology 256 (3) (2010) 879–886, https://doi.org/10.1148/radiol.10091162.
[119] L.S. Babiarz, B. Astor, M.A. Mohamed, B.A. Wasserman, Comparison of gadolinium-enhanced cardiovascular magnetic resonance angiography with high-resolution black blood cardiovascular magnetic resonance for assessing carotid artery stenosis, J. Cardiovasc. Magn. Reson. 9 (1) (2007) 63–70, https://doi.org/10.1080/10976640600843462.
[120] J.M. Cai, T.S. Hatsukami, M.S. Ferguson, R. Small, N.L. Polissar, C. Yuan, Classification of human carotid atherosclerotic lesions with in vivo multicontrast magnetic resonance imaging, Circulation 106 (11) (2002) 1368–1373, https://doi.org/10.1161/01.CIR.0000028591.44554.F9.
[121] L. Saba, A.R. Moody, T. Saam, et al., Vessel wall-imaging biomarkers of carotid plaque vulnerability in stroke prevention trials: a viewpoint from the carotid imaging consensus group, JACC Cardiovasc. Imag. 13 (11) (2020) 2445–2456, https://doi.org/10.1016/j.jcmg.2020.07.046.
[122] L. Saba, T. Saam, H.R. Jäger, et al., Imaging biomarkers of vulnerable carotid plaques for stroke risk prediction and their potential clinical implications, Lancet Neurol. 18 (6) (2019) 559–572, https://doi.org/10.1016/S1474-4422(19)30035-3.
[123] L. Saba, W. Brinjikji, J.D. Spence, et al., Roadmap consensus on carotid artery plaque imaging and impact on therapy strategies and guidelines: an international, multispecialty, expert review and position statement, AJNR Am. J. Neuroradiol. 42 (9) (2021) 1566–1575, https://doi.org/10.3174/ajnr.A7223.
[124] V.C. Cappendijk, K.B.J.M. Cleutjens, S. Heeneman, et al., In vivo detection of hemorrhage in human atherosclerotic plaques with magnetic resonance imaging, J. Magn. Reson. Imag. 20 (1) (2004) 105–110, https://doi.org/10.1002/jmri.20060.
[125] A. Schindler, R. Schinner, N. Altaf, et al., Prediction of stroke risk by detection of hemorrhage in carotid plaques: meta-analysis of individual patient data, JACC Cardiovasc. Imag. 13 (2 Pt 1) (2020) 395–406, https://doi.org/10.1016/j.jcmg.2019.03.028.
[126] H. Kamel, A.E. Merkler, C. Iadecola, A. Gupta, B.B. Navi, Tailoring the approach to embolic stroke of undetermined source: a review, JAMA Neurol. 76 (7) (2019) 855–861, https://doi.org/10.1001/jamaneurol.2019.0591.
[127] H. Kamel, B.B. Navi, A.E. Merkler, et al., Reclassification of ischemic stroke etiological subtypes on the basis of high-risk nonstenosing carotid plaque, Stroke 51 (2) (2020) 504–510, https://doi.org/10.1161/STROKEAHA.119.027970.
[128] H. Baradaran, P. Patel, G. Gialdini, et al., Quantifying intracranial internal carotid artery stenosis on MR angiography, AJNR Am. J. Neuroradiol. 38 (5) (2017) 986–990, https://doi.org/10.3174/ajnr.A5113.
[129] T. Hirai, Y. Korogi, K. Ono, et al., Prospective evaluation of suspected stenoocclusive disease of the intracranial artery: combined MR angiography and CT angiography compared with digital subtraction angiography, AJNR Am. J. Neuroradiol. 23 (1) (2002) 93–101.
[130] A.J. Degnan, G. Gallagher, Z. Teng, J. Lu, Q. Liu, J.H. Gillard, MR angiography and imaging for the evaluation of middle cerebral artery atherosclerotic disease, AJNR Am. J. Neuroradiol. 33 (8) (2012) 1427–1435, https://doi.org/10.3174/ajnr.A2697.
[131] V.T. Lehman, W. Brinjikji, D.F. Kallmes, et al., Clinical interpretation of high-resolution vessel wall MRI of intracranial arterial diseases, Br. J. Radiol. 89 (1067) (2016), 20160496, https://doi.org/10.1259/bjr.20160496.
[132] A. Lindenholz, A.G. van der Kolk, J.J.M. Zwanenburg, J. Hendrikse, The use and pitfalls of intracranial vessel wall imaging: how we do it, Radiology 286 (1) (2018) 12–28, https://doi.org/10.1148/radiol.2017162096.
[133] D.M. Mandell, M. Mossa-Basha, Y. Qiao, et al., Intracranial vessel wall MRI: principles and expert consensus recommendations of the American society of neuroradiology, AJNR Am. J. Neuroradiol. 38 (2) (2017) 218–229, https://doi.org/10.3174/ajnr.A4893.
[134] Y. Wang, X. Liu, X. Wu, A.J. Degnan, A. Malhotra, C. Zhu, Culprit intracranial plaque without substantial stenosis in acute ischemic stroke on vessel wall MRI: a systematic review, Atherosclerosis 287 (2019) 112–121, https://doi.org/10.1016/j.atherosclerosis.2019.06.907.
[135] M. Zhao, S. Amin-Hanjani, S. Ruland, A.P. Curcio, L. Ostergren, F.T. Charbel, Regional cerebral blood flow using quantitative MR angiography, AJNR Am. J. Neuroradiol. 28 (8) (2007) 1470–1473, https://doi.org/10.3174/ajnr.A0582.
[136] T. Wehrum, I. Dragonu, C. Strecker, et al., Aortic atheroma as a source of stroke - assessment of embolization risk using 3D CMR in stroke patients and controls, J. Cardiovasc. Magn. Reson. Off. J. Soc. Cardiovasc. Magn. Reson. 19 (1) (2017) 67, https://doi.org/10.1186/s12968-017-0379-x.
[137] M.S. Cocker, J.D. Spence, R. Hammond, et al., [(18)F]-NaF PET/CT identifies active calcification in carotid plaque, JACC Cardiovasc. Imag. 10 (4) (2017) 486–488, https://doi.org/10.1016/j.jcmg.2016.03.005.
[138] N.R. Evans, J.M. Tarkin, E.P. Le, et al., Integrated cardiovascular assessment of atherosclerosis using PET/MRI, Br. J. Radiol. 93 (1113) (2020), 20190921, https://doi.org/10.1259/bjr.20190921.
[139] M. Aizaz, R.P.M. Moonen, J.A.J. van der Pol, C. Prieto, R.M. Botnar, M.E. Kooi, PET/MRI of atherosclerosis, Cardiovasc. Diagn. Ther. 10 (4) (2020) 1120–1139, https://doi.org/10.21037/cdt.2020.02.09.
[140] J.H.F. Rudd, E.A. Warburton, T.D. Fryer, et al., Imaging atherosclerotic plaque inflammation with [18F]-fluorodeoxyglucose positron emission tomography, Circulation 105 (23) (2002) 2708–2711, https://doi.org/10.1161/01.cir.0000020548.60110.76.
[141] J. Bucerius, F. Hyafil, H.J. Verberne, et al., Position paper of the cardiovascular committee of the European association of nuclear medicine (EANM) on PET imaging of atherosclerosis, Eur. J. Nucl. Med. Mol. Imag. 43 (4) (2016) 780–792, https://doi.org/10.1007/s00259-015-3259-3.
[142] M.S. Cocker, J.D. Spence, R. Hammond, et al., [18F]-Fluorodeoxyglucose PET/CT imaging as a marker of carotid plaque inflammation: comparison to immunohistology and relationship to acuity of events, Int. J. Cardiol. 271 (2018) 378–386, https://doi.org/10.1016/j.ijcard.2018.05.057.
[143] R.M. Kwee, M.T.B. Truijman, W.H. Mess, et al., Potential of integrated [^{18}F] fluorodeoxyglucose positron-emission tomography/CT in identifying vulnerable carotid plaques, Am. J. Neuroradiol. 32 (5) (2011) 950–954, https://doi.org/10.3174/ajnr.A2381.
[144] S. Chaker, K. Al-Dasuqi, H. Baradaran, et al., Carotid plaque positron emission tomography imaging and cerebral ischemic disease, Stroke 50 (8) (2019) 2072–2079, https://doi.org/10.1161/STROKEAHA.118.023987.

[145] P. Poredos, A. Spirkoska, L. Lezaic, M.B. Mijovski, M.K. Jezovnik, Patients with an inflamed atherosclerotic plaque have increased levels of circulating inflammatory markers, J. Atherosclerosis Thromb. 24 (1) (2017) 39–46, https://doi.org/10.5551/jat.34884.
[146] M.K. Jezovnik, N. Zidar, L. Lezaic, B. Gersak, P. Poredos, Identification of inflamed atherosclerotic lesions in vivo using PET-CT, Inflammation 37 (2) (2014) 426–434, https://doi.org/10.1007/s10753-013-9755-3.
[147] M.T.B. Truijman, R.M. Kwee, R.H.M. van Hoof, et al., Combined 18F-FDG PET-CT and DCE-MRI to assess inflammation and microvascularization in atherosclerotic plaques, Stroke 44 (12) (2013) 3568–3570, https://doi.org/10.1161/STROKEAHA.113.003140.
[148] J. Wang, H. Liu, J. Sun, et al., Varying correlation between 18F-fluorodeoxyglucose positron emission tomography and dynamic contrast-enhanced MRI in carotid atherosclerosis: implications for plaque inflammation, Stroke 45 (6) (2014) 1842–1845, https://doi.org/10.1161/STROKEAHA.114.005147.
[149] J.M. Tarkin, F.R. Joshi, N.R. Evans, et al., Detection of atherosclerotic inflammation by (68)Ga-DOTATATE PET compared to [(18)F]FDG PET imaging, J. Am. Coll. Cardiol. 69 (14) (2017) 1774–1791, https://doi.org/10.1016/j.jacc.2017.01.060.
[150] O. Gaemperli, J. Shalhoub, D.R.J. Owen, et al., Imaging intraplaque inflammation in carotid atherosclerosis with 11C-PK11195 positron emission tomography/computed tomography, Eur. Heart J. 33 (15) (2012) 1902–1910, https://doi.org/10.1093/eurheartj/ehr367.
[151] S. Vöö, R.M. Kwee, J.C. Sluimer, et al., Imaging intraplaque inflammation in carotid atherosclerosis with 18F-fluorocholine positron emission tomography-computed tomography: prospective study on vulnerable atheroma with immunohistochemical validation, Circ. Cardiovasc. Imaging 9 (5) (2016), https://doi.org/10.1161/CIRCIMAGING.115.004467.
[152] A.T. Vesey, W.S.A. Jenkins, A. Irkle, et al., 18)F-Fluoride and (18)F-fluorodeoxyglucose positron emission tomography after transient ischemic attack or minor ischemic stroke: case-control study, Circ. Cardiovasc. Imaging 10 (3) (2017), e004976, https://doi.org/10.1161/CIRCIMAGING.116.004976.
[153] N.V. Joshi, A.T. Vesey, M.C. Williams, et al., 18F-fluoride positron emission tomography for identification of ruptured and high-risk coronary atherosclerotic plaques: a prospective clinical trial, Lancet (London, England) 383 (9918) (2014) 705–713, https://doi.org/10.1016/S0140-6736(13)61754-7.
[154] K.T.M. Mizuno, Coronary angioscopy, Springer Japan, https://books.google.com/books?id=b7MYCgAAQBAJ.
[155] Y. Uchida, Recent advances in coronary angioscopy, J. Cardiol. 57 (1) (2011) 18–30, https://doi.org/10.1016/j.jjcc.2010.11.001.
[156] L.E. Savastano, E.J. Seibel, Scanning fiber angioscopy: a multimodal intravascular imaging platform for carotid atherosclerosis, Neurosurgery 64 (CN_suppl_1) (2017) 188–198, https://doi.org/10.1093/neuros/nyx322.
[157] L.E. Savastano, Q. Zhou, A. Smith, et al., Multimodal laser-based angioscopy for structural, chemical and biological imaging of atherosclerosis, Nat. Biomed. Eng. 1 (2) (2017) 23, https://doi.org/10.1038/s41551-016-0023.
[158] P. Kan, M. Mokin, A.A. Abla, et al., Utility of intravascular ultrasound in intracranial and extracranial neurointerventions: experience at university at buffalo neurosurgery-millard fillmore gates circle hospital, Neurosurg. Focus 32 (1) (2012) E6, https://doi.org/10.3171/2011.10.FOCUS11242.
[159] G. Sangiorgi, F. Bedogni, P. Sganzerla, et al., The Virtual histology in CaroTids Observational RegistrY (VICTORY) study: a European prospective registry to assess the feasibility and safety of intravascular ultrasound and virtual histology during carotid interventions, Int. J. Cardiol. 168 (3) (2013) 2089–2093, https://doi.org/10.1016/j.ijcard.2013.01.159.
[160] E.B. Diethrich, M. Pauliina Margolis, D.B. Reid, et al., Virtual histology intravascular ultrasound assessment of carotid artery disease: the Carotid Artery Plaque Virtual Histology Evaluation (CAPITAL) study, J. Endovasc. Ther.: Off. J. Int. Soc. Endovasc. Spec. 14 (5) (2007) 676–686, https://doi.org/10.1177/152660280701400512.
[161] N. Funatsu, Y. Enomoto, Y. Egashira, et al., Tissue protrusion with attenuation is associated with ischemic brain lesions after carotid artery stenting, Stroke 51 (1) (2020) 327–330, https://doi.org/10.1161/STROKEAHA.119.026332.
[162] G. de Donato, E. Pasqui, G. Alba, et al., Clinical considerations and recommendations for OCT-guided carotid artery stenting, Expert Rev. Cardiovasc Ther. 18 (4) (2020) 219–229, https://doi.org/10.1080/14779072.2020.1756777.
[163] G.A. Roth, C. Johnson, A. Abajobir, et al., Global, regional, and national burden of cardiovascular diseases for 10 causes, 1990 to 2015, J. Am. Coll. Cardiol. 70 (1) (2017) 1–25, https://doi.org/10.1016/j.jacc.2017.04.052.
[164] V.L. Feigin, B. Norrving, G.A. Mensah, Global burden of stroke, Circ. Res. 120 (3) (2017) 439–448, https://doi.org/10.1161/CIRCRESAHA.116.308413.
[165] R. Cau, V. Cherchi, G. Micheletti, et al., Potential role of artificial intelligence in cardiac magnetic resonance imaging, J. Thorac. Imag. (3) (2021) 142–148, https://doi.org/10.1097/rti.0000000000000584. Publish Ah.
[166] R. Cau, G. Faa, V. Nardi, et al., Long-COVID diagnosis: from diagnostic to advanced AI-driven models, Eur. J. Radiol. 148 (January) (2022), 110164, https://doi.org/10.1016/j.ejrad.2022.110164.
[167] D. Shishikura, Noninvasive imaging modalities to visualize atherosclerotic plaques, Cardiovasc. Diagn. Ther. 6 (4) (2016) 340–353, https://doi.org/10.21037/cdt.2015.11.07.
[168] K.I. Paraskevas, A.N. Nicolaides, S.K. Kakkos, Asymptomatic carotid stenosis and risk of stroke (ACSRS) study: what have we learned from it? Ann. Transl. Med. 8 (19) (2020) 1271, https://doi.org/10.21037/atm.2020.02.156.
[169] S.K. Kakkos, M.B. Griffin, A.N. Nicolaides, et al., The size of juxtaluminal hypoechoic area in ultrasound images of asymptomatic carotid plaques predicts the occurrence of stroke, J. Vasc. Surg. 57 (3) (2013) 608–609, https://doi.org/10.1016/j.jvs.2012.09.045.
[170] Y.-T. Shen, L. Chen, W.-W. Yue, H.-X. Xu, Artificial intelligence in ultrasound, Eur. J. Radiol. 139 (2021), 109717, https://doi.org/10.1016/j.ejrad.2021.109717.
[171] C. Boyd, G. Brown, T. Kleinig, et al., Machine learning quantitation of cardiovascular and cerebrovascular disease: a systematic review of clinical applications, Diagnostics (Basel, Switzerland) 11 (3) (2021) 551, https://doi.org/10.3390/diagnostics11030551.
[172] M. Biswas, L. Saba, S. Chakrabartty, et al., Two-stage artificial intelligence model for jointly measurement of atherosclerotic wall thickness and plaque burden in carotid ultrasound: a screening tool for cardiovascular/stroke risk assessment, Comput. Biol. Med. 123 (2020), 103847, https://doi.org/10.1016/j.compbiomed.2020.103847.
[173] L. Saba, S.S. Sanagala, S.K. Gupta, et al., Ultrasound-based internal carotid artery plaque characterization using deep learning paradigm on a supercomputer: a cardiovascular disease/stroke risk assessment system, Int. J. Cardiovasc. Imag. 37 (5) (2021) 1511–1528, https://doi.org/10.1007/s10554-020-02124-9.
[174] M. Biswas, V. Kuppili, T. Araki, et al., Deep learning strategy for accurate carotid intima-media thickness measurement: an ultrasound study on Japanese diabetic cohort, Comput. Biol. Med. 98 (2018) 100–117, https://doi.org/10.1016/j.compbiomed.2018.05.014.
[175] P.K. Jain, N. Sharma, A.A. Giannopoulos, L. Saba, A. Nicolaides, J.S. Suri, Hybrid deep learning segmentation models for atherosclerotic plaque in internal carotid artery B-mode ultrasound, Comput. Biol. Med. 136 (2021), 104721, https://doi.org/10.1016/j.compbiomed.2021.104721.
[176] C.-A. Cheng, H.-W. Chiu, An artificial neural network model for the evaluation of carotid artery stenting prognosis using a national-wide database, in: Annu Int Conf IEEE Eng Med Biol Soc IEEE Eng Med Biol Soc Annu Int Conf 2017, 2017, pp. 2566–2569, https://doi.org/10.1109/EMBC.2017.8037381.
[177] J.P. Jeon, C. Kim, B.-D. Oh, S.J. Kim, Y.-S. Kim, Prediction of persistent hemodynamic depression after carotid angioplasty and stenting using artificial neural network model, Clin. Neurol. Neurosurg. 164 (2018) 127–131, https://doi.org/10.1016/j.clineuro.2017.12.005.
[178] L. Saba, A. Jamthikar, D. Gupta, et al., Global perspective on carotid intima-media thickness and plaque: should the current measurement guidelines be revisited? Int. Angiol. 38 (6) (2019) 451–465, https://doi.org/10.23736/S0392-9590.19.04267-6.
[179] U.R. Acharya, S.V. Sree, M.R.K. Mookiah, et al., Computed tomography carotid wall plaque characterization using a combination of discrete wavelet transform and texture features: a pilot study, Proc. Inst. Mech. Eng. Part H J Eng Med 227 (6) (2013) 643–654, https://doi.org/10.1177/0954411913480622.
[180] F.L. Caetano dos Santos, M. Kolasa, M. Terada, J. Salenius, H. Eskola, M. Paci, VASIM: an automated tool for the quantification of carotid atherosclerosis by computed tomography angiography, Int. J. Cardiovasc. Imag. 35 (6) (2019) 1149–1159, https://doi.org/10.1007/s10554-019-01549-1.
[181] U. Hanning, P.B. Sporns, M.N. Psychogios, et al., Imaging-based prediction of histological clot composition from admission CT imaging, Published online January, J. Neurointerventional Surg. 22 (2021), https://doi.org/10.1136/neurintsurg-2020-016774. neurintsurg-2020-016774.
[182] E.P.V. Le, N.R. Evans, J.M. Tarkin, et al., Contrast CT classification of asymptomatic and symptomatic carotids in stroke and transient ischaemic attack with deep learning and interpretability, Eur. Heart J. 41 (Supplement_2) (2020), https://doi.org/10.1093/ehjci/ehaa946.2418.
[183] B.K. Lal, V.S. Kashyap, J.B. Patel, et al., Novel application of artificial intelligence algorithms to develop a predictive model for major adverse neurologic events in patients with carotid atherosclerosis, J. Vasc. Surg. 72 (1) (2020) e176–e177, https://doi.org/10.1016/j.jvs.2020.04.306.
[184] J. Wu, J. Xin, X. Yang, et al., Deep morphology aided diagnosis network for segmentation of carotid artery vessel wall and diagnosis of carotid atherosclerosis on black-blood vessel wall MRI, Med. Phys. 46 (12) (2019) 5544–5561, https://doi.org/10.1002/mp.13739.
[185] D.D. Samber, S. Ramachandran, A. Sahota, et al., Segmentation of carotid arterial walls using neural networks, World J. Radiol. 12 (1) (2020) 1–9, https://doi.org/10.4329/wjr.v12.i1.1.
[186] L. Chen, J. Sun, G. Canton, et al., Automated artery localization and vessel wall segmentation using tracklet refinement and polar conversion, IEEE Access Pract. Innov. Open Solut. 8 (2020) 217603–217614, https://doi.org/10.1109/access.2020.3040616.
[187] N. Balu, V.L. Yarnykh, B. Chu, J. Wang, T. Hatsukami, C. Yuan, Carotid plaque assessment using fast 3D isotropic resolution black-blood MRI, Magn. Reson. Med. 65 (3) (2011) 627–637, https://doi.org/10.1002/mrm.22642.
[188] L. Chen, H. Zhao, H. Jiang, et al., Domain adaptive and fully automated carotid artery atherosclerotic lesion detection using an artificial intelligence approach (LATTE) on 3D MRI, Magn. Reson. Med. 86 (3) (2021) 1662–1673, https://doi.org/10.1002/mrm.28794.
[189] Y. Dong, Y. Pan, X. Zhao, R. Li, C. Yuan, W. Xu, Identifying carotid plaque composition in MRI with convolutional neural networks, in: IEEE International Conference on Smart Computing, SMARTCOMP, 2017, pp. 1–8, https://doi.org/10.1109/SMARTCOMP.2017.7947015, 2017.
[190] R. Zhang, Q. Zhang, A. Ji, et al., Identification of high-risk carotid plaque with MRI-based radiomics and machine learning, Eur. Radiol. 31 (5) (2021) 3116–3126, https://doi.org/10.1007/s00330-020-07361-z.
[191] J. Wang, P. Börnert, H. Zhao, et al., Simultaneous noncontrast angiography and intraplaque hemorrhage (SNAP) imaging for carotid atherosclerotic disease evaluation, Magn. Reson. Med. 69 (2) (2013) 337–345, https://doi.org/10.1002/mrm.24254.

[192] I. Koktzoglou, R. Huang, A.L. Ong, P.J. Aouad, E.A. Aherne, R.R. Edelman, Feasibility of a sub-3-minute imaging strategy for ungated quiescent interval slice-selective MRA of the extracranial carotid arteries using radial k-space sampling and deep learning-based image processing, Magn. Reson. Med. 84 (2) (2020) 825–837, https://doi.org/10.1002/mrm.28179.
[193] M. Ziegler, J. Alfraeus, M. Bustamante, et al., Automated segmentation of the individual branches of the carotid arteries in contrast-enhanced MR angiography using DeepMedic, BMC Med. Imag. 21 (1) (2021) 38, https://doi.org/10.1186/s12880-021-00568-6.
[194] A. Tang, R. Tam, A. Cadrin-Chênevert, et al., Canadian association of radiologists white paper on artificial intelligence in radiology, Can. Assoc. Radiol. J. = J l'Association Can des Radiol. 69 (2) (2018) 120–135, https://doi.org/10.1016/j.carj.2018.02.002.
[195] P. Lambin, E. Rios-Velazquez, R. Leijenaar, et al., Radiomics: extracting more information from medical images using advanced feature analysis, Eur. J. Cancer 48 (4) (2012) 441–446, https://doi.org/10.1016/j.ejca.2011.11.036.
[196] ESR, R. ES of, White paper on imaging biomarkers, Insights Imaging 1 (2) (2010) 42–45, https://doi.org/10.1007/s13244-010-0025-8.
[197] E. Neri, M. Del Re, F. Paiar, et al., Radiomics and liquid biopsy in oncology: the holons of systems medicine, Insights Imaging 9 (6) (2018) 915–924, https://doi.org/10.1007/s13244-018-0657-7.
[198] K. Doi, Computer-aided diagnosis in medical imaging: historical review, current status and future potential, Comput. Med. Imag. Graph. 31 (4–5) (2007) 198–211, https://doi.org/10.1016/j.compmedimag.2007.02.002.
[199] C.M. Micheel, S.J. Nass, G.S. Omenn (Eds.), Committee on the Review of Omics-Based Tests for Predicting Patient Outcomes in Clinical Trials, 2012, https://doi.org/10.17226/13297.
[200] V. Kumar, Y. Gu, S. Basu, et al., Radiomics: the process and the challenges, Magn. Reson. Imaging 30 (9) (2012) 1234–1248, https://doi.org/10.1016/j.mri.2012.06.010.
[201] H.J.W.L. Aerts, The potential of radiomic-based phenotyping in precision medicine: a review, JAMA Oncol. 2 (12) (2016) 1636–1642, https://doi.org/10.1001/jamaoncol.2016.2631.
[202] R.J. Gillies, P.E. Kinahan, H. Hricak, Radiomics: images are more than pictures, they are data, Radiology 278 (2) (2016) 563–577, https://doi.org/10.1148/radiol.2015151169.
[203] S.S.F. Yip, H.J.W.L. Aerts, Applications and limitations of radiomics, Phys. Med. Biol. 61 (13) (2016) R150–R166, https://doi.org/10.1088/0031-9155/61/13/R150.
[204] B. Ambale-Venkatesh, X. Yang, C.O. Wu, et al., Cardiovascular event prediction by machine learning: the multi-ethnic study of atherosclerosis, Circ. Res. 121 (9) (2017) 1092–1101, https://doi.org/10.1161/CIRCRESAHA.117.311312.
[205] D. Han, K.K. Kolli, S.J. Al'Aref, et al., Machine learning framework to identify individuals at risk of rapid progression of coronary atherosclerosis: from the PARADIGM registry, J. Am. Heart Assoc. 9 (5) (2020), e013958, https://doi.org/10.1161/JAHA.119.013958.
[206] X. Hu, P.D. Reaven, A. Saremi, et al., Machine learning to predict rapid progression of carotid atherosclerosis in patients with impaired glucose tolerance, EURASIP J. Bioinf. Syst. Biol. 2016 (1) (2016) 14, https://doi.org/10.1186/s13637-016-0049-6.
[207] M. Motwani, D. Dey, D.S. Berman, et al., Machine learning for prediction of all-cause mortality in patients with suspected coronary artery disease: a 5-year multicentre prospective registry analysis, Eur. Heart J. 38 (7) (2017) 500–507, https://doi.org/10.1093/eurheartj/ehw188.
[208] J.A. Quesada, A. Lopez-Pineda, V.F. Gil-Guillén, et al., Machine learning to predict cardiovascular risk, Int. J. Clin. Pract. 73 (10) (2019), e13389, https://doi.org/10.1111/ijcp.13389.
[209] J.W. Groenendyk, N.N. Mehta, Applying the ordinal model of atherosclerosis to imaging science: a brief review, Open Hear 5 (2) (2018), e000861, https://doi.org/10.1136/openhrt-2018-000861.
[210] O. Terrada, B. Cherradi, A. Raihani, O. Bouattane, A novel medical diagnosis support system for predicting patients with atherosclerosis diseases, Inform. Med. Unlocked 21 (2020), 100483, https://doi.org/10.1016/j.imu.2020.100483.
[211] A.R. van Rosendael, G. Maliakal, K.K. Kolli, et al., Maximization of the usage of coronary CTA derived plaque information using a machine learning based algorithm to improve risk stratification; insights from the CONFIRM registry, J Cardiovasc. Comput. Tomogr. 12 (3) (2018) 204–209, https://doi.org/10.1016/j.jcct.2018.04.011.
[212] S.F. Weng, J. Reps, J. Kai, J.M. Garibaldi, N. Qureshi, Can machine-learning improve cardiovascular risk prediction using routine clinical data? PLoS One 12 (4) (2017), e0174944 https://doi.org/10.1371/journal.pone.0174944.
[213] R.S. Cires-Drouet, M. Mozafarian, A. Ali, S. Sikdar, B.K. Lal, Imaging of high-risk carotid plaques: ultrasound, Semin. Vasc. Surg. 30 (1) (2017) 44–53, https://doi.org/10.1053/j.semvascsurg.2017.04.010.
[214] V. Rafailidis, D.Y. Huang, G.T. Yusuf, P.S. Sidhu, General principles and overview of vascular contrast-enhanced ultrasonography, Ultrasonics (Guildf.) 39 (1) (2020) 22–42, https://doi.org/10.14366/usg.19022.
[215] T. Wannarong, G. Parraga, D. Buchanan, et al., Progression of carotid plaque volume predicts cardiovascular events, Stroke 44 (7) (2013) 1859–1865, https://doi.org/10.1161/STROKEAHA.113.001461.
[216] M. Kuk, T. Wannarong, V. Beletsky, G. Parraga, A. Fenster, J.D. Spence, Volume of carotid artery ulceration as a predictor of cardiovascular events, Stroke 45 (5) (2014) 1437–1441, https://doi.org/10.1161/STROKEAHA.114.005163.
[217] A. Madani, V. Beletsky, A. Tamayo, C. Munoz, J.D. Spence, High-risk asymptomatic carotid stenosis: ulceration on 3D ultrasound vs TCD microemboli, Neurology 77 (8) (2011) 744–750, https://doi.org/10.1212/WNL.0b013e31822b0090.
[218] K.P.H. Nies, L.J.M. Smits, M. Kassem, P.J. Nederkoorn, R.J. van Oostenbrugge, M. E. Kooi, Emerging role of carotid MRI for personalized ischemic stroke risk prediction in patients with carotid artery stenosis, Front. Neurol. 12 (2021), 718438, https://doi.org/10.3389/fneur.2021.718438.
[219] M. Kassem, A. Florea, F.M. Mottaghy, R. van Oostenbrugge, M.E. Kooi, Magnetic resonance imaging of carotid plaques: current status and clinical perspectives, Ann. Transl. Med. 8 (19) (2020) 1266, https://doi.org/10.21037/atm-2020-cass-16.
[220] H. Baradaran, P.K. Myneni, P. Patel, et al., Association between carotid artery perivascular fat density and cerebrovascular ischemic events, J. Am. Heart Assoc. 7 (24) (2018), e010383, https://doi.org/10.1161/JAHA.118.010383.
[221] H. Baradaran, L.B. Eisenmenger, P.J. Hinckley, et al., Optimal carotid plaque features on computed tomography angiography associated with ischemic stroke, J. Am. Heart Assoc. 10 (5) (2021), e019462, https://doi.org/10.1161/JAHA.120.019462.
[222] J. Sun, Y. Song, H. Chen, et al., Adventitial perfusion and intraplaque hemorrhage: a dynamic contrast-enhanced MRI study in the carotid artery, Stroke 44 (4) (2013) 1031–1036, https://doi.org/10.1161/STROKEAHA.111.000435.
[223] K.I. Paraskevas, J.D. Spence, F.J. Veith, A.N. Nicolaides, Identifying which patients with asymptomatic carotid stenosis could benefit from intervention, Stroke 45 (12) (2014) 3720–3724, https://doi.org/10.1161/STROKEAHA.114.006912.
[224] A.R. Naylor, J.-B. Ricco, G.J. de Borst, et al., Editor's choice - management of atherosclerotic carotid and vertebral artery disease: 2017 clinical practice guidelines of the European society for vascular Surgery (ESVS), Eur. J. Vasc. Endovasc. Surg. Off. J. Eur. Soc. Vasc. Surg. 55 (1) (2018) 3–81, https://doi.org/10.1016/j.ejvs.2017.06.021.
[225] L. Saba, M. Mossa-Basha, A. Abbott, et al., Multinational survey of current practice from imaging to treatment of atherosclerotic carotid stenosis, Cerebrovasc. Dis. 50 (1) (2021) 108–120, https://doi.org/10.1159/000512181.
[226] K.I. Paraskevas, D.P. Mikhailidis, H. Baradaran, et al., Management of patients with asymptomatic carotid stenosis may need to Be individualized: a multidisciplinary call for action, J. Stroke 23 (2) (2021) 202–212, https://doi.org/10.5853/jos.2020.04273.